LEBANESE AMERICAN UNIVERSITY

Mathematical Modeling of Atherosclerosis

By

Elissa A. Salloum

A thesis
Submitted in partial fulfillment of the
requirements
for the degree of Master of Science in
Applied and Computational Mathematics

School of Arts and Science

May 2021

©2021

Elissa A. Salloum

All Rights Reserved

LAU
الجامعة اللبنانية الأميركية
Lebanese American University

THESIS APPROVAL FORM

Student Name: Elissa Salloum I.D. #: 201905955

Thesis Title: **Mathematical Modeling of Atherosclerosis** as an Inflammation.

Program: **Applied and Computational Mathematics**

Department: **Computer Science and Mathematics**

School: **Arts and Sciences**

The undersigned certify that they have examined the final electronic copy of this thesis and approved it in Partial Fulfillment of the requirements for the degree of: **master** in the major of Applied and Computational Mathematics.

Thesis Advisor's Name: Nader El Khatib

Signature: [redacted] Date: 01 / 06 / 2021
Day Month Year

Committee Member's Name: Chadi Nour

Signature: [redacted] Date: 01 / 06 / 2021
Day Month Year

Committee Member's Name: Jean Takche

Signature: [redacted] Date: 01 / 06 / 2021
Day Month Year

ii

LAU
الجامعة اللبنانية الأميركية
Lebanese American University

THESIS COPYRIGHT RELEASE FORM

LEBANESE AMERICAN UNIVERSITY NON-EXCLUSIVE DISTRIBUTION LICENSE

By signing and submitting this license, you (the author(s) or copyright owner) grants the Lebanese American University (LAU) the non-exclusive right to reproduce, translate (as defined below), and/or distribute your submission (including the abstract) worldwide in print and electronic formats and in any medium, including but not limited to audio or video. You agree that LAU may, without changing the content, translate the submission to any medium or format for the purpose of preservation. You also agree that LAU may keep more than one copy of this submission for purposes of security, backup and preservation. You represent that the submission is your original work, and that you have the right to grant the rights contained in this license. You also represent that your submission does not, to the best of your knowledge, infringe upon anyone's copyright. If the submission contains material for which you do not hold copyright, you represent that you have obtained the unrestricted permission of the copyright owner to grant LAU the rights required by this license, and that such third-party owned material is clearly identified and acknowledged within the text or content of the submission. IF THE SUBMISSION IS BASED UPON WORK THAT HAS BEEN SPONSORED OR SUPPORTED BY AN AGENCY OR ORGANIZATION OTHER THAN LAU, YOU REPRESENT THAT YOU HAVE FULFILLED ANY RIGHT OF REVIEW OR OTHER OBLIGATIONS REQUIRED BY SUCH CONTRACT OR AGREEMENT. LAU will clearly identify your name(s) as the author(s) or owner(s) of the submission, and will not make any alteration, other than as allowed by this license, to your submission.

Name: **Elissa Salloum**

Signature

Date: **10-5-2021**

LAU
الجامعة اللبنانية الأميركية
Lebanese American University

PLAGIARISM POLICY COMPLIANCE STATEMENT

I certify that:

1. I have read and understood LAU's Plagiarism Policy.
2. I understand that failure to comply with this Policy can lead to academic and disciplinary actions against me.
3. This work is substantially my own, and to the extent that any part of this work is not my own I have indicated that by acknowledging its sources.

Name: Elissa Salloum

Signature 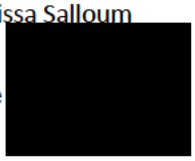

Date: 10-5-2021

To my Precious Family and Friends.

Acknowlegment

This thesis would not have been possible without the support of many people to whom I am grateful.
First, I would like to thank the thesis advisor, Dr. Nader El Khatib for his endless encouragement especially during these challenging times of pandemic. I am profoundly grateful to work with such a professional and dedicated advisor .
Another special thanks to my committee members, Dr. Chadi Nour and Dr. Jean Takchi for their contribution and guidance.

I am also very thankful to my precious family for always offering support and love. I could not accomplish my ambitions without them.
Finally I would like to thank all my friends for their moral support to me and especially my beloved friend Ghada Abi Younes that has accompanied me since the beginning of my thesis.

Mathematical Modeling of Atherosclerosis as an Inflammation

Elissa A. Salloum

ABSTRACT

In this thesis, we suggest a one and two dimensional mathematical models of reaction-diffusion type that study the inflammatory process of atherosclerosis in the intima. They consider the concentration of five main agents: LDL, free radicals, oxidized LDL, macrophages and cytokines.
The existence and stability analysis of fixed points for the kinetic system is performed. All obtained results are analyzed and compared to those in [1] in order to provide an appropriate biological interpretation.
We prove the existence of solution of traveling wave type which decribes the set up of the inflammatory reaction as a reaction–diffusion wave inside the intima. This result is shown theoretically and numerically. We prove as well the convergence of the 2D model to the 1D case in the thin domain.

Keywords: Atherosclerosis, PDE, Mathematical Modeling, Traveling Waves, Numerical Simulations.

Table of Contents

List of Figures **ix**

List of Tables **x**

1 Introduction **1**
1.1 Introduction 1
1.2 Biological Process 1

2 Mathematical Modeling of Atherosclerosis in the Literature **4**

3 One Dimensional Model **7**
3.1 Model Description 7
3.2 Mathematical Analysis 8
3.2.1 Kinetic System 8
3.2.2 Equilibrium Points 9
3.2.3 Stability Analysis 12
3.3 Biological Interpretation 15

4 Existence and Numerical Simulations of Traveling Waves for the 1D case **17**
4.1 Reduction of the System 17
4.2 Existence of Traveling Waves 18
4.3 Numerical Simulations 18

5 Two Dimensional Model **21**
5.1 Model Description 21
5.2 Boundary Conditions Scaling 22
5.3 Reduction of the System 23
5.4 Numerical Simulations 23

6 Conclusion **27**

References **29**

A Computations **30**

B Simulations **33**

List of Figures

1.1 The number of deaths by cause in the World between 2000 and 2017. The top cause of deaths is due to Cardivascular diseases. In addition, the total number of deaths has increased from 13.7 million in 2000 to 17.79 million in 2017. 2
1.2 Difference between normal human artery and artery narrowed by atherosclerotic plaque. 2

3.1 The case where E_0 is the unique fixed point 11
3.2 In this case, there are two fixed points: E_0 and E_1. 11
3.3 The case of existence of three fixed points: E_0, E_1 and E_u. 12
3.4 Stability analysis simulation for case 1. 14
3.5 Stability analysis simulation for case 2. 14
3.6 Stability analysis simulation for case 3. 15

4.1 In the monostable case, we notice that even a small perturbation of the non-inflammatory state will lead to the propagation of a chronic inflammatory reaction. 19
4.2 A small perturbation of the non-inflammatory state will not lead to the propagation of a chronic inflammatory reaction. 19
4.3 A large perturbation of the non-inflammatory state will lead to the propagation of a chronic inflammatory reaction. 20

5.1 Geometry of the rectangular domain. 22
5.2 In the monostable case, we notice that even a small perturbation of the non-inflammatory state will lead to the set up of a chronic inflammatory reaction. Moreover, the solution very weakly depends on y. Left: Solution at $t = 0$. Right: Solution at $t = 8.2$. 24
5.3 We observe that the solution weakly depends on y. In addition, a large perturbation of the noninflammatory state will lead to the set of an inflammatory reaction. Left: Solution at $t = 0$. Right: Solution at $t = 20$. 25
5.4 Similarly, the solution weakly depends on y. Besides, a small perturbation of the noninflammatory state will not lead to the set up of a chronic inflammatory reaction. Left: Initial condition. Right: Subsequent time. 26

List of Tables

3.1 Stability of fixed points. 15
3.2 Biological meaning of the conditions. 16

Chapter 1

Introduction

1.1 Introduction

According to the World Health Organization, cardiovascular diseases, the most devastating consequences of atherosclerosis, are the world's leading cause of death. By virtue of adopting a Western life-style, epidemiological studies indicate that the prevalence of atherosclerosis is rising all over the world and is prone to reach epidemic proportions in the upcoming decades [2].
In 2017, Cardiovascular diseases were responsible for approximately 17.79 million deaths worldwide (based on Fig. (1.1)). Furthermore, at global level, total deaths from cardiovascular diseases increased by an estimated 21.1% between 2007 and 2017. However, death rates decreased from 259.9 deaths per 100 000 in 2007 to 233.1 per 100 000 in 2017 [3].
Despite the progress made in diagnosis, surgical treatment and control of high cholesterol level, so far, significant progress in order to fight atherosclerosis remains unfulfilled [4].

1.2 Biological Process

Definition of Atherosclerosis

"Atherosclerosis" comes from the ancient Greek words where "athero" means gruel or accumulation of lipids and "sclerosis" means hardness, and is hardening of the arteries.
It's is a chronic inflammatory disease characterized by the buildup of cholesterol and other fatty deposits, called plaques, within the arterial wall. This buildup leads to restricted blood flow through narrowing the blood vessel lumen leading to various clinical syndromes such as heart attacks and strokes [6].

Endothelium Dysfunction and LDL Penetration

Based on experimental and clinical studies, it is proved that under the impact of many well-known risk factors, such as smoking, diabetes, hypertension, dyslipidemia, etc. endothelial cells become dysfunctional [8].
Increased focal permeability of the luminal endothelium may account for an increased focal accumulation of lipoproteins. In particular, low density lipoproteins

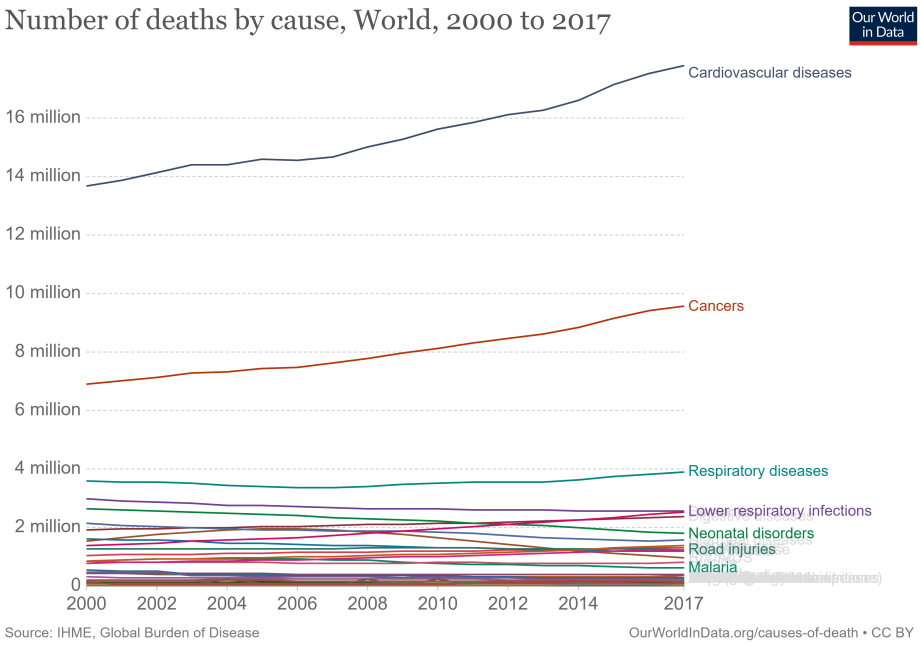

Figure 1.1: The number of deaths by cause in the World between 2000 and 2017. The top cause of deaths is due to Cardivascular diseases. In addition, the total number of deaths has increased from 13.7 million in 2000 to 17.79 million in 2017. [5]

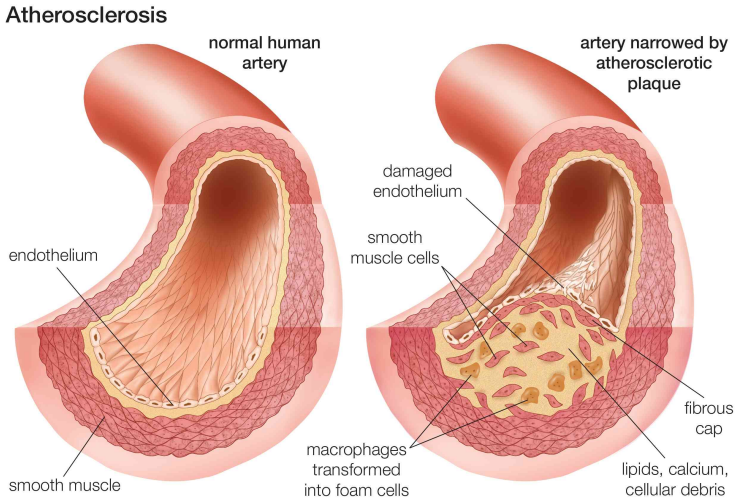

Figure 1.2: Difference between normal human artery and artery narrowed by atherosclerotic plaque. [7]

(LDL) circulating in the bloodstream, accumulate in the intima and once trapped in the arterial wall, LDL particles are prone to modifications. [9].
One of such modifications is the oxidation process of LDL particles. It is the outcome of an excess of free radicals and other oxidant species [10]. In addition, LDL oxidation is less likely to take place in the plasma by reason of the highly efficient antioxidant defense mechanisms of human plasma. Whereas they are more exposed to oxidation processes once they become trapped inside the artery. [11].

Immune Response

Oxidized LDL (ox-LDL) are very toxic and recognized by the immune system as foreign substances. The immune system will be stimulated and release chemoattractants that mediate the adhesion of immune cells such as monocytes circulating in the blood.
The adherence of monocytes to the endothelium and their migration into the arterial wall are mediated by the presence of cellular adhesion molecules on the surface of endothelial cells. Subsequently, monocytes migrate across the endothelium into the subendothelial space of the arterial intima where they differentiate into macrophages [9].

Macrophages take up the ox-LDL and become filled with cholesterol which transform them into lipid-filled foam cells.
The accumulation of modified LDL within the intima triggers an inflammatory response in the nearby endothelial cells. Macrophages release pro-inflammatory cytokines which in turn promote the recruitment of new immune cells [12]. On the other hand, macrophages produce anti-inflammatory cytokines that inhibit the production of pro-inflammatory cytokines.

A progressive recruitment of immune cells, and a continuous uptake of ox-LDL, leads to the formation of a large number of foam cells, hence a fatty streak is formed [11].
Accordingly, smooth muscle cells will migrate from the media to the intima to create a fibrous cap that covers the lipid deposit. This fibrous cap isolates the lipid deposit from the blood flow.
Fatty streaks can form as early as during childhood and meanwhile the person may remain asymptomatic. In certain situations, they may regress over time and eventually disappear. Alternatively, they can continue to grow and lead to various clinical manifestations [11].

Stable and Unstable Plaque

One can distinguish between several types of plaques where some of them are more likely to rupture than the others.
The stable plaques are unlikely to rupture due to their thick fibrous cap with a small lipid core area.
However, unstable and vulnerable plaques are characterized by a thin fibrous cap where their lipid core is substantial.
If plaque ruptures, it will either lead to the blockage of the oxygenated blood from reaching the brain or it will bleed. This causes the brain cells to die [13].

Chapter 2

Mathematical Modeling of Atherosclerosis in the Literature

In this chapter, we present a brief review on different research studies performed on mathematical models for the atherosclerosis inflammatory process. In fact many reseachers have been working on this topic within the last decades.

- In reference [1], the authors studied the inflammatory process by developing a one- and two- dimensional models of reaction-diffusion equations. As an important result, the concentration of the ox-LDL in the intima plays a crucial role: low ox-LDL concentrations do not lead to a chronic inflammatory reaction, intermediate concentrations of ox-LDL corresponds to a bistable system where a chronic inflammatory reaction may set up, but for that it has to overcome a threshold. High concentrations of ox-LDL represent a monostable case where even a small perturbation of the non-inflammatory case leads to a travelling wave propagation which corresponds to a chronic inflammatory response.

- In reference [14], the authors proposed a 2D mathematical model of the initiation and development of atherosclerosis considering the concentration of blood cells inside the intima and of pro- and anti-inflammatory cytokines. The proposed model is of reaction-diffusion type equipped with nonlinear boundary conditions, it describes the recruitment of monocytes as a function of the concentration of inflammatory cytokines. They proved the existence of travelling waves and confirm their previous results that atherosclerosis develops as a reaction-diffusion wave. Moreover, the theoretical results are verified by the numerical simulations.

- In reference [15], the authors represented a simplified model of ordinary differential equations that explores the role of the inflammation. The model takes into account two main lesion constituents: cholesterol-carrying modified Low Density Lipoproteins and macrophage foam cells. The main result is that macrophage proliferation and constant signaling to the endothelial cells, rather than an increasing influx of modified LDL, that drives lesion instability.

- In [16], a mathematical model of varying sophistication for different stages of atherosclerosis is developed. An initial attempt is made in order to

have estimates of the various parameter values characterizing the system. All developed models employ the 'large artery hypothesis' that blood is a Newtonian fluid and that a kinematic viscosity is known. Further, the issue of wall shear stress in cap degradation is discussed, the idea of an oscillating shear index is introduced followed by a discussion whether existing ideas on wound healing is applicable to plaque rupture.

- In [17], the point is to examine complex dynamics associated with the plaque growth in human arteries which leads to fatal consequences to human life. For the mathematical analysis, different techniques are employed such as the theory of dynamical systems, bifurcation analysis, numerical analysis etc. In this work, atherosclerosis is considered as a coupled problem for both blood flow conditions and biochemical evolution of the plaque constituents involved. In addition, the authors explore the interaction of various important plaque constituents on short time scales, and its accumulation into the artery on a longer time scale to be able to distinguish which factors are the most relevant and what can be inferred from a mathematical perspective.

- In [18], the authors modeled the atherosclerosis plaque formation using a system of reaction-diffusion equations. They first provided a 1D model of lesion growth and then perform numerical simulations on an idealized 2D geometry of the carotid artery bifurcation before and after the formation of the atherosclerotic plaque. For that purpose, blood is considered as an incompressible non-Newtonian fluid with shear-thinning viscosity. Moreover, they presented a study of the wall shear stress and blood velocity behavior in a geometry with one plaque and also with two plaques in different positions.

- In reference [4], the studied mathematical model considers cells and cytokines of innate immunity. It describes a chronic inflammatory response in the intima of an artery vessel wall. The authors investigated stationary points and studied their stability for reduced kinetic systems of two and five ODE's. The relationship of the obtained results is analyzed in order to give an appropriate biological interpretation.

- In reference [19], a spatially resolved and quantitative mathematical model of key contributors of early atherosclerosis is developed. It combines Darcy's law for the transmural flow through vessels walls, the Kedem-Katchalsky equations for endothelial fluxes of lipoproteins, a quantitative model of early plaque formation and a novel submodel for macrophage recruitment. Via the parameterization and analysis of the model, the authors suggested that the advective flux of lipoproteins through the endothelium is decisive, however the influence of the advective transport within the artery wall is negligible. Moreover, they concluded that regions in arteries with an approximate wall shear stress exposure below 20% of the average exposure and their surroundings are potential regions where progression-prone atherosclerotic plaques develop.

- In reference [20], a mathematical model of important chemical processes leading to atherosclerotic plaque development is studied and analyzed. It

considers the concentrations of LDLs, oxidized LDLs, foam cells, oxidized LDL-derived chemoattractant and macrophage-derived chemoattractant, the density of macrophages, smooth muscle cells (SMCs), and extracellular matrix (ECM). The authors found the positive invariant set and study local stability. Further, oscillatory behavior of the model solutions is investigated. Numerical solutions show various dynamic behaviors that can occur under suitable conditions on the system parameters.

- In [21], the authors studied a 1D atherosclerosis model of reaction-diffusion system of three equations, equipped with homogeneous Neumann boundary conditions. The method of upper and lower solutions and its associated monotone iteration are used in order to establish existence, uniqueness and boundedness of global solutions for the time dependent problem and as well for the corresponding steady-state solutions. They studied the stability of constant steady-state solutions and the asymptotic behavior of the time-dependent solutions.

In this thesis, a mathematical model for the atherosclerosis inflammatory process has been achieved inspired from previous modeling techniques and by applying some modifications.

Chapter 3

One Dimensional Model

3.1 Model Description

We construct the following mathematical model for the atherosclerosis inflammatory process on an interval representing the intima. It considers LDL, free-radicals, ox-LDL, immune cells and cytokines concentrations.
Below is the model that consists of a system of five coupled partial differential equations of reaction-diffusion type for $x \in [\,0, L]$ and $t \in [\,0, \infty[\,$.
Furthermore, we impose at the boundaries a homogeneous Neumann boundary condition.

$$\begin{cases} \dfrac{\partial L}{\partial t} = d_L \dfrac{\partial^2 L}{\partial x^2} + \sigma_L - s_L r L - \lambda_L L \\ \dfrac{\partial r}{\partial t} = d_r \dfrac{\partial^2 r}{\partial x^2} + \sigma_r - s_L r L - \lambda_r r \\ \dfrac{\partial L_{ox}}{\partial t} = d_{L_{ox}} \dfrac{\partial^2 L_{ox}}{\partial x^2} + s_L r L - \lambda_{L_{ox}} L_{ox} \\ \dfrac{\partial M}{\partial t} = d_M \dfrac{\partial^2 M}{\partial x^2} + \dfrac{\alpha_1 L_{ox} + \beta_1 A}{1 + \frac{A}{\tau_1}} - \lambda_M M \\ \dfrac{\partial A}{\partial t} = d_A \dfrac{\partial^2 A}{\partial x^2} + \dfrac{\alpha_2 A M}{1 + \frac{A}{\tau_2}} - \lambda_A A \end{cases} \tag{3.1}$$

- The first term of the right hand side in each equation is a diffusion term.
- The first equation models the evolution of the concentration of LDL in time, where σ_L is a constant source of LDL supplied by the blood, $-s_L r L$ corresponds to the loss of LDL via their oxidation and by their reaction with free radicals and $-\lambda_L L$ represents the degradation of LDL particles.
- The second equation models the evolution of free radicals concentration. σ_r is the source of free radicals in the intima, $-s_L r L$ is defined similarly as in the previous equation and $-\lambda_r r$ corresponds to the degradation of free radicals.
- The third equation describes the evolution of ox-LDL concentration through time. Here, $s_L r L$ corresponds to the production of ox-LDL mediated by the

oxidation of LDL particles. $-\lambda_{L_{ox}} L_{ox}$ corresponds to the loss of ox-LDL due their degradation and their uptake by the immune cells.

- The fourth equation models the evolution of the concentration of macrophages. The term $\dfrac{\alpha_1 L_{ox} + \beta_1 A}{1 + \frac{A}{\tau_1}}$ models the recruitment of immune cells from the blood flow promoted by pro-inflammatory cytokines. Here, $\alpha_1 L_{ox}$ corresponds to the beginning of the inflammation, that is the recruitment of monocytes due to the presence of ox-LDL, $\beta_1 A$ corresponds to the auto-amplification of the recruitment immune cells due to the pro-inflammatory cytokines. The denominator $1 + \dfrac{A}{\tau_1}$ represents the mechanical saturation of the recruitment of M, that is the effect of the fibrous cap created by smooth muscle cells, with τ_1 being the characteristic time for the fibrous cap formation. The last term $-\lambda_M M$ refers to the degradation of immune cells along with their differentiation into foam cells.

- The last equation models the evolution pro-inflammatory cytokines concentration. $\dfrac{\alpha_2 AM}{1 + \frac{A}{\tau_2}}$ refers to the pro-inflammatory cytokines production rate where $\alpha_2 AM$ designates the secretion of pro-inflammatory cytokines promoted by pro-inflammatory cytokines themselves and the denominator $1 + \dfrac{A}{\tau_2}$ corresponds to the inhibition of pro-inflammatory cytokines secretion mediated by anti-inflammatory cytokines, with τ_2 being the necessary time for the inhibition to act. The last term $-\lambda_A A$ refers to the degradation of cytokines.

3.2 Mathematical Analysis

Our main goal is to gain an understanding of the behaviors of the solutions to the systems, for that, we study the existence of equilibrium points of the kinetic system and then analyse their stability.

3.2.1 Kinetic System

The kinetic system considers only the reaction part of the system of Eqs.(3.1) so the system turns into coupled ordinary differential equations defined in Eq.(3.2)

$$\begin{cases} \dfrac{dL}{dt} = \sigma_L - s_L r L - \lambda_L L \\ \dfrac{dr}{dt} = \sigma_r - s_L r L - \lambda_r r \\ \dfrac{dL_{ox}}{dt} = s_L r L - \lambda_{L_{ox}} L_{ox} \\ \dfrac{dM}{dt} = \dfrac{\alpha_1 L_{ox} + \beta_1 A}{1 + \frac{A}{\tau_1}} - \lambda_M M \\ \dfrac{dA}{dt} = \dfrac{\alpha_2 AM}{1 + \frac{A}{\tau_2}} - \lambda_A A \end{cases} \tag{3.2}$$

Buckingham's Pi theorem is applied in order to obtain simpler equations with a reduced number of parameters. The number of parameters decreased from 13 to 10 so the equations are easier to deal with. The detailed computations are presented in appendix A.
The dimensionless system becomes:

$$\begin{cases} \dfrac{dL}{dt} = \sigma_L - s_L r L - \lambda_L L \\ \dfrac{dr}{dt} = \sigma_r - s_L r L - \lambda_r r \\ \dfrac{dL_{ox}}{dt} = s_L r L - \lambda_{L_{ox}} L_{ox} \\ \dfrac{dM}{dt} = \dfrac{\alpha_1 L_{ox} + \beta_1 A}{1 + A} - \lambda_M M \\ \dfrac{dA}{dt} = \dfrac{AM}{1 + \frac{A}{\tau_2}} - A \end{cases} \tag{3.3}$$

3.2.2 Equilibrium Points

Definition 3.2.1 *Equilibria of an autonomous system of the form:* $\dfrac{dX}{dt} = F(X)$ *are obtained by solving the system* $F(X) = 0$

In order to determine the equilibrium points of system (3.3), the system of Eqs. (3.4) is solved by looking for nonnegative solutions:

$$\begin{cases} \sigma_L - s_L r L - \lambda_L L = 0 \\ \sigma_r - s_L r L - \lambda_r r = 0 \\ s_L r L - \lambda_{L_{ox}} L_{ox} = 0 \\ \dfrac{\alpha_1 L_{ox} + \beta_1 A}{1 + A} - \lambda_M M = 0 \\ \dfrac{AM}{1 + \frac{A}{\tau_2}} - A = 0 \end{cases} \tag{3.4}$$

$L^* = \dfrac{\sigma_L - \sigma_r + \lambda_r r^*}{\lambda_L}$, $r^* = \dfrac{s_L\sigma_r - s_L\sigma_L - \lambda_r\lambda_L + \sqrt{(s_L\sigma_L + \lambda_r\lambda_L - s_L\sigma_r)^2 + 4 s_L\lambda_r\sigma_r\lambda_L}}{2 s_L\lambda_r}$
and $L^*_{ox} = \dfrac{\gamma}{\lambda_{L_{ox}}}$ with $\gamma = s_L r^* L^*$ are respectively the unique solutions of the first three equations of the system (3.4).

Now Eqs. (3.5) and (3.6) can be solved by including the solution of L_{ox} that have been solved within the first three equations of system (3.4)

$$\frac{\alpha_1 L^*_{ox} + \beta_1 A}{1 + A} - \lambda_M M = 0 \tag{3.5}$$

$$\frac{AM}{1 + \frac{A}{\tau_2}} - A = 0 \tag{3.6}$$

We notice that Eq. (3.6) generates two solutions: either $A = 0$ or $M = 1 + \frac{A}{\tau_2}$

Remark 3.2.1 *In the following, we impose the condition:*

$$\beta_1 - \alpha_1 L_{ox}^* > 0 \tag{3.7}$$

This condition ensures the existence of traveling wave solution in Chap. 4

Nullclines on the plane $A = 0$

Using Eq. (3.5) with $A = 0$, we get: $M_0 = \frac{\alpha_1}{\lambda_M} L_{ox}^* = \frac{\alpha_1 \gamma}{\lambda_M \lambda_{L_{ox}}}$
From that, we deduce the existence of the fixed point E_0 with $E_0 = (L^*, r^*, L_{ox}^*, M_0, 0)$

Nullclines on the plane $M = 1 + \frac{A}{\tau_2}$

From Eqs. (3.5) and (3.6), we get:

$$\begin{cases} M = g_1(A) = \frac{1}{\lambda_M}(\frac{\alpha_1 L_{ox}^* + \beta_1 A}{1 + A}) \\ M = g_2(A) = 1 + \frac{A}{\tau_2} \end{cases}$$

Fixed points are obtained by solving $g_1(A) = g_2(A)$. Three different cases are obatined and represented (Details in appendix A).

<u>**Case 1:**</u> Either $\frac{\alpha_1 \gamma}{\lambda_M \lambda_{L_{ox}}} < \frac{\beta_1}{\lambda_M} \leq 1$
or $\frac{\alpha_1 \gamma}{\lambda_M \lambda_{L_{ox}}} < 1 < \frac{\beta_1}{\lambda_M}$ and $0 < \tau_2 < \frac{1}{(1 - \frac{\beta_1}{\lambda_M})^2} \left(\sqrt{1 - \frac{\alpha_1 \gamma}{\lambda_M \lambda_{L_{ox}}}} + \sqrt{\frac{\beta_1}{\lambda_M} - \frac{\alpha_1 \gamma}{\lambda_M \lambda_{L_{ox}}}} \right)^2$
or $\frac{\alpha_1 \gamma}{\lambda_M \lambda_{L_{ox}}} = 1 \geq \frac{\beta_1}{\lambda_M}$
or $\frac{\alpha_1 \gamma}{\lambda_M \lambda_{L_{ox}}} = 1 < \frac{\beta_1}{\lambda_M}$ and $0 < \tau_2 \leq \frac{1}{\frac{\beta_1}{\lambda_M} - 1}$

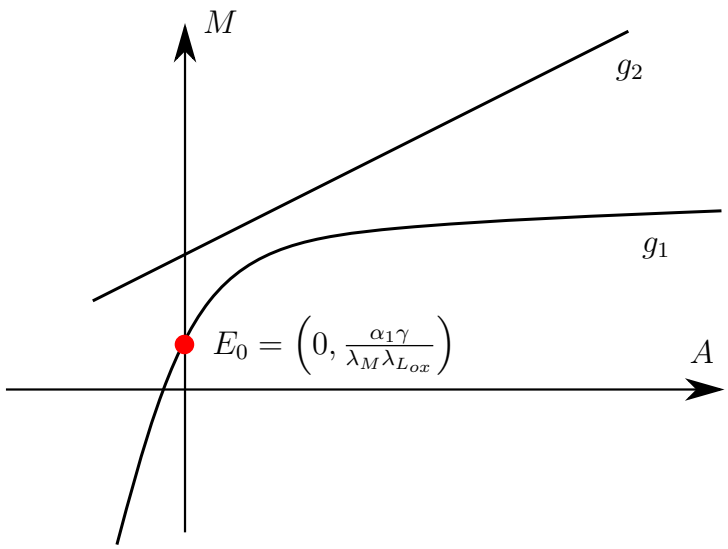

Figure 3.1: The case where E_0 is the unique fixed point

Case 2: Either $\dfrac{\alpha_1\gamma}{\lambda_M\lambda_{L_{ox}}} > 1$

or $\dfrac{\alpha_1\gamma}{\lambda_M\lambda_{L_{ox}}} < 1 < \dfrac{\beta_1}{\lambda_M}$ and $\tau_2 = \dfrac{1}{(1-\frac{\beta_1}{\lambda_M})^2}\left(\sqrt{1-\dfrac{\alpha_1\gamma}{\lambda_M\lambda_{L_{ox}}}} + \sqrt{\dfrac{\beta_1}{\lambda_M} - \dfrac{\alpha_1\gamma}{\lambda_M\lambda_{L_{ox}}}}\right)^2$

or $\dfrac{\alpha_1\gamma}{\lambda_M\lambda_{L_{ox}}} = 1 < \dfrac{\beta_1}{\lambda_M}$ and $\tau_2 > \dfrac{1}{\frac{\beta_1}{\lambda_M} - 1}$

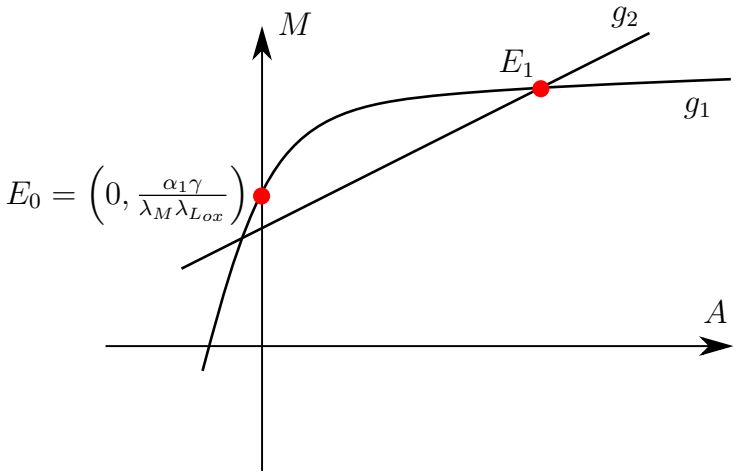

Figure 3.2: In this case, there are two fixed points: E_0 and E_1.

Case 3:

$\dfrac{\alpha_1\gamma}{\lambda_M\lambda_{L_{ox}}} < 1 < \dfrac{\beta_1}{\lambda_M}$ and $\dfrac{1}{(1-\frac{\beta_1}{\lambda_M})^2}\left(\sqrt{1-\dfrac{\alpha_1\gamma}{\lambda_M\lambda_{L_{ox}}}} + \sqrt{\dfrac{\beta_1}{\lambda_M} - \dfrac{\alpha_1\gamma}{\lambda_M\lambda_{L_{ox}}}}\right)^2 < \tau_2$

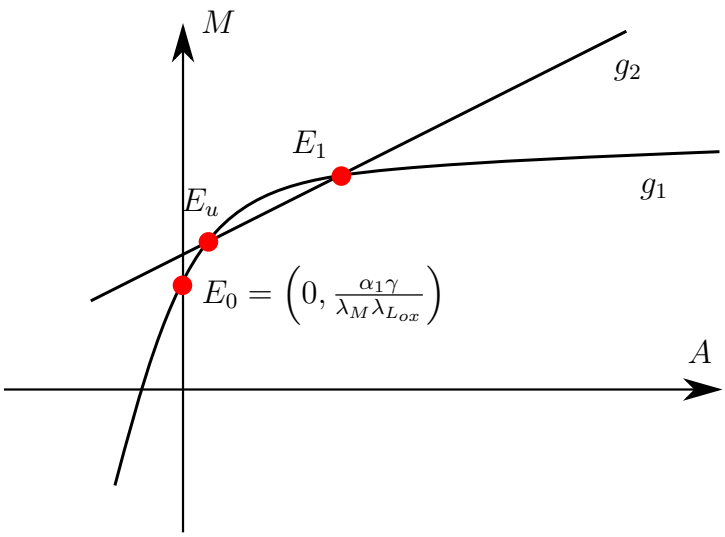

Figure 3.3: The case of existence of three fixed points: E_0, E_1 and E_u.

3.2.3 Stability Analysis

In this part, we study the stability of the fixed points E_0, E_1 and E_u whenever they exist.
The Jacobian matrix of the system of Eqs. (3.3) is given by:

$$J = \begin{bmatrix} -s_L r - \lambda_L & -s_L L & 0 & 0 & 0 \\ -s_L r & -s_L L - \lambda_r & 0 & 0 & 0 \\ s_L r & s_L L & -\lambda_{L_{ox}} & 0 & 0 \\ 0 & 0 & \frac{\alpha_1}{1+A} & -\lambda_M & \frac{\beta_1 - \alpha_1 L_{ox}}{(1+A)^2} \\ 0 & 0 & 0 & \frac{A}{1+\frac{A}{\tau_2}} & \frac{M}{(1+\frac{A}{\tau_2})^2} - 1 \end{bmatrix} \tag{3.8}$$

Stability of E_0

The stability of E_0 is done by solving: $det(J_{E_0} - \lambda I) = 0$, i.e by solving the following determinant for λ.

$$\begin{vmatrix} -s_L r^* - \lambda_L - \lambda & -s_L L^* & 0 & 0 & 0 \\ -s_L r^* & -s_L L^* - \lambda_r - \lambda & 0 & 0 & 0 \\ s_L r^* & s_L L^* & -\lambda_{L_{ox}} - \lambda & 0 & 0 \\ 0 & 0 & \alpha_1 & -\lambda_M - \lambda & \beta_1 - \alpha_1 L^*_{ox} \\ 0 & 0 & 0 & 0 & M_0 - 1 - \lambda \end{vmatrix} = 0$$

We clearly notice that E_0 is stable if $M_0 < 1$, i.e $\dfrac{\alpha_1\gamma}{\lambda_M\lambda_{L_{ox}}} < 1$. Otherwise E_0 is unstable.
In addition, E_0 is always stable in the plane $A = 0$.
In cases 1 and 3, $p = \tau_2\left(1 - \dfrac{\alpha_1\gamma}{\lambda_M\lambda_{L_{ox}}}\right) > 0$, hence E_0 is stable.

However, in case 2, $p = \tau_2 \left(1 - \dfrac{\alpha_1 \gamma}{\lambda_M \lambda_{L_{ox}}}\right) < 0$, consequently, E_0 is unstable.
(Refer to p in appendix A)

Remark 3.2.2 *The study for the stability of the fixed points E_1 and E_u can be simply reduced to the following jacobian matrix:*

$$J' = \begin{bmatrix} -\lambda_M & \dfrac{\beta_1 - \alpha_1 L^*_{ox}}{(1+A)^2} \\ \dfrac{A}{1+\frac{A}{\tau_2}} & \dfrac{M}{(1+\frac{A}{\tau_2})^2} - 1 \end{bmatrix} = \begin{bmatrix} -\lambda_M & \lambda_M g_1'(A) \\ \dfrac{A}{1+\frac{A}{\tau_2}} & \dfrac{1}{1+\frac{A}{\tau_2}} - 1 \end{bmatrix}$$

Stability of E_1

From Figs. (3.2) and (3.3), we notice that $g_1'(E_1) < g_2'(E_1) = \dfrac{1}{\tau_2}$.
Hence $det(J'_{E_1}) = \dfrac{-\lambda_M}{1+\frac{A_1}{\tau_2}} + \lambda_M - \dfrac{\lambda_M A_1 g_1'(A_1)}{1+\frac{A_1}{\tau_2}} > 0$
In addition, $tr(J'_{E_1}) = -\lambda_M - 1 + \dfrac{1}{1+\frac{A_1}{\tau_2}} < 0$
Thus all eigenvalues are negative and E_1 is always stable whenever it exists.

Stability of E_u

From Fig. (3.3), we deduce that $g_1'(E_u) > g_2'(E_u) = \dfrac{1}{\tau_2}$.
Hence $det(J'_{E_u}) = \dfrac{-\lambda_M}{1+\frac{A_u}{\tau_2}} + \lambda_M - \dfrac{\lambda_M A_u g_1'(A_u)}{1+\frac{A_u}{\tau_2}} < 0$
Thus one of the eigenvalues is positive and hence E_u is always unstable whenever it exists.

We illustrate below figures of the stability analysis simulations for all the cases in the AM-plane.

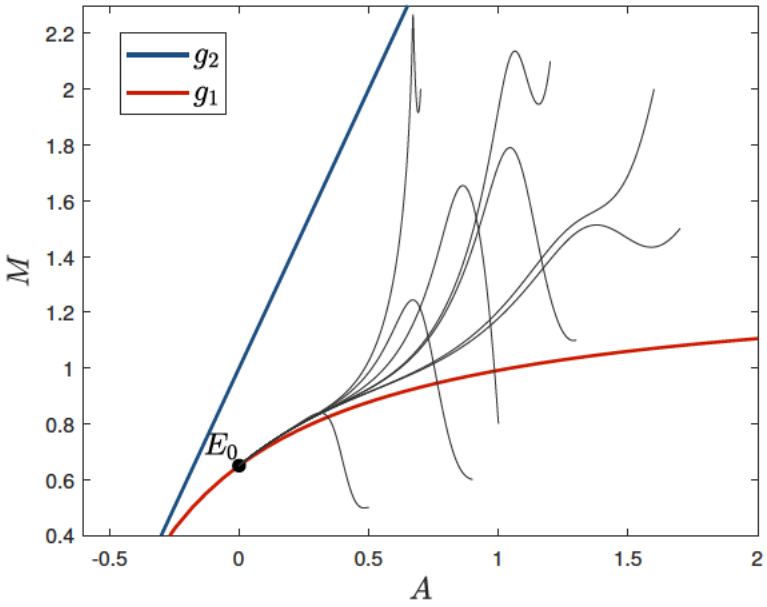

Figure 3.4: Stability analysis simulation for case 1.

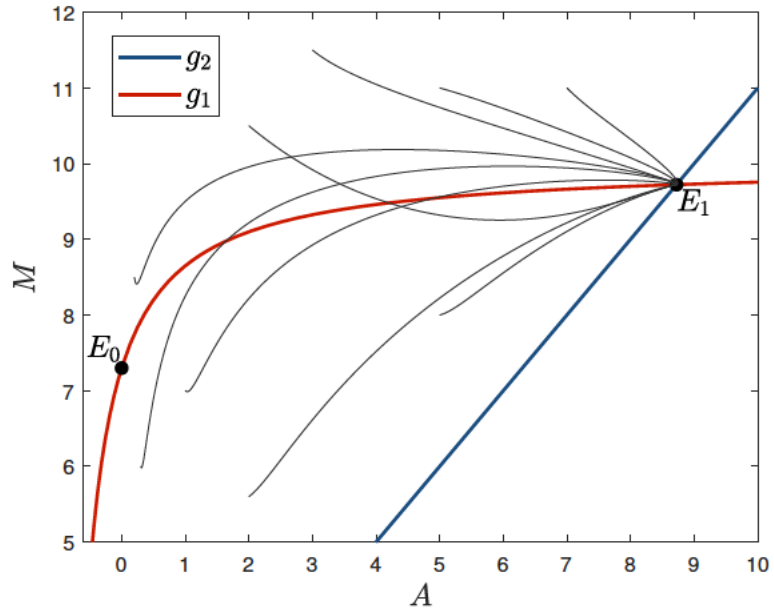

Figure 3.5: Stability analysis simulation for case 2.

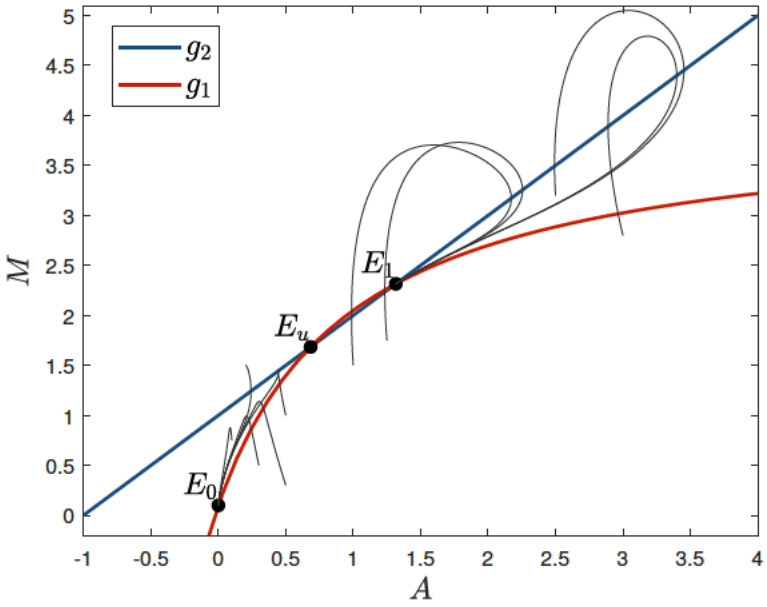

Figure 3.6: Stability analysis simulation for case 3.

All the obtained results for the stability analysis are summarized in Table (3.1)

Case	$\mathbf{E_0}$	$\mathbf{E_1}$	$\mathbf{E_u}$
1	Stable	-	-
2	Stable in the plane $A = 0$	Stable	-
3	Stable	Stable	Unstable

Table 3.1: Stability of fixed points.

3.3 Biological Interpretation

We deduce from the preceding section that the system admits at most three equilibrium points having the following biological interpretation:

- E_0 corresponds to the non-inflammatory state where no cytokines are elaborated even in the presence of ox-LDL and immune cells. Hence no inflammation is triggered.
- E_1 corresponds to the inflammatory state. At this stage, the concentrations of macrophages and cytokines are large regardless of the concentration of ox-LDL. For that, it causes the set up of the inflammation.
- E_u is an intermediate equilibrium point, it is always unstable whenever it exists. It characterizes a threshold to overcome in order to move from the non inflammatory state E_0 to the inflammatory state E_1.

The biological interpretation is given in terms of γ, i.e the ox-LDL concentration in the intima.
Table (3.2) gives the biological meaning for each condition in terms of γ.

Conditions	Consequence	Significance
$\frac{\alpha_1\gamma}{\lambda_M\lambda_{L_{ox}}} < \frac{\beta_1}{\lambda_M} \leq 1$	γ small	Low concentration of ox-LDL
$\frac{\alpha_1\gamma}{\lambda_M\lambda_{L_{ox}}} < 1 < \frac{\beta_1}{\lambda_M}$ and $0 < \tau_2 < \frac{1}{(1-\frac{\beta_1}{\lambda_M})^2}\left(\sqrt{1-\frac{\alpha_1\gamma}{\lambda_M\lambda_{L_{ox}}}}+\sqrt{\frac{\beta_1}{\lambda_M}-\frac{\alpha_1\gamma}{\lambda_M\lambda_{L_{ox}}}}\right)^2$	γ small	Low concentration of ox-LDL
$\frac{\alpha_1\gamma}{\lambda_M\lambda_{L_{ox}}} = 1 \geq \frac{\beta_1}{\lambda_M}$	γ small	Low concentration of ox-LDL
$\frac{\alpha_1\gamma}{\lambda_M\lambda_{L_{ox}}} = 1 < \frac{\beta_1}{\lambda_M}$ and $0 < \tau_2 \leq \frac{1}{\frac{\beta_1}{\lambda_M}-1}$	γ small	Low concentration of ox-LDL
$\frac{\alpha_1\gamma}{\lambda_M\lambda_{L_{ox}}} < 1 < \frac{\beta_1}{\lambda_M}$ and $\frac{1}{(1-\frac{\beta_1}{\lambda_M})^2}\left(\sqrt{1-\frac{\alpha_1\gamma}{\lambda_M\lambda_{L_{ox}}}}+\sqrt{\frac{\beta_1}{\lambda_M}-\frac{\alpha_1\gamma}{\lambda_M\lambda_{L_{ox}}}}\right)^2 < \tau_2$	γ intermediate	Intermediate concentration of ox-LDL
$\frac{\alpha_1\gamma}{\lambda_M\lambda_{L_{ox}}} > 1$	γ large	Large concentration of ox-LDL
$\frac{\alpha_1\gamma}{\lambda_M\lambda_{L_{ox}}} < 1 < \frac{\beta_1}{\lambda_M}$ and $\tau_2 = \frac{1}{(1-\frac{\beta_1}{\lambda_M})^2}\left(\sqrt{1-\frac{\alpha_1\gamma}{\lambda_M\lambda_{L_{ox}}}}+\sqrt{\frac{\beta_1}{\lambda_M}-\frac{\alpha_1\gamma}{\lambda_M\lambda_{L_{ox}}}}\right)^2$	γ large	Large concentration of ox-LDL
$\frac{\alpha_1\gamma}{\lambda_M\lambda_{L_{ox}}} = 1 < \frac{\beta_1}{\lambda_M}$ and $\tau_2 > \frac{1}{\frac{\beta_1}{\lambda_M}-1}$	γ large	Large concentration of ox-LDL

Table 3.2: Biological meaning of the conditions.

Moreover, the concentration of ox-LDL in the intima depends on two other important components that play a crucial role in atherosclerosis: σ_L the source of low-density lipoproteins in the intima and σ_r the source of free-radicals that causes the oxidation of LDL particles.
In addition, γ is relative to σ_L and σ_r, i.e the more sources of LDL and free radicals lead to more ox-LDL particles in the intima. This concept is explained in appendix A.
We finally conclude the following biological interpretation:

- If γ is small hence no inflammation is triggered. This exactly explains the stability of the unique fixed point E_0.

- If γ is intermediate, we have two stable equilibrium points E_0 and E_1 and an unstable one E_u. This corresponds to the bistable case where E_u represents a threshold to overcome in order to move from the non-inflammatory state E_0 to the inflammatory one E_1. Hence the development of the atherosclerotic plaque arises if the initial conditions are large enough, otherwise the system will reach E_0 and no chronic inflammatory reaction is set up.

- If γ is large, there are two equilibrium points: E_0 is unstable and E_1 is stable. This corresponds to the monostable case and the fact that γ is large explains the stability of E_1. Hence even a small perturbation of the non-inflammatory state will lead to the set up of an inflammation.

Chapter 4

Existence and Numerical Simulations of Traveling Waves for the 1D case

The goal in this chapter is to describe the set up of the inflammatory reaction as a traveling wave inside the intima. For this purpose, we set up the conditions for the propagation of the chronic inflammatory reaction, accompanied by numerical simulations that describe the wave propagation. Note that macrophages and cytokines are the main agents that lead to the formation of the atherosclerotic plaque.

4.1 Reduction of the System

We notice that in the system of Eqs. (3.1), the first three equations consist of functions that are independent from the variables M and A. Therefore, they can be solved altogether independently of the last two equations. Consequently, the solution $L_{ox}(x,t)$ can be replaced in the fourth equation so we are able to reduce the study of existence of traveling wave solution to the following system:

$$\begin{cases} \dfrac{\partial M}{\partial t} = d_M \dfrac{\partial^2 M}{\partial x^2} + \dfrac{\alpha_1 L_{ox} + \beta_1 A}{1 + \frac{A}{\tau_1}} - \lambda_M M \\ \dfrac{\partial A}{\partial t} = d_A \dfrac{\partial^2 A}{\partial x^2} + \dfrac{\alpha_2 A M}{1 + \frac{A}{\tau_2}} - \lambda_A A \end{cases} \tag{4.1}$$

where $L_{ox}(x,t)$ is known.
Its dimensionless kinetic system is defined by:

$$\begin{cases} \dfrac{dM}{dt} = \dfrac{\alpha_1 L_{ox} + \beta_1 A}{1 + A} - \lambda_M M \\ \dfrac{dA}{dt} = \dfrac{AM}{1 + \frac{A}{\tau_2}} - A \end{cases} \tag{4.2}$$

The study of existence and stability of fixed points remains exactly the same as in parts (3.2.2) and (3.2.3).

The Jacobian matrix of system (4.2) becomes as follows:

$$J^* = \begin{bmatrix} -\lambda_M & \dfrac{\beta_1 - \alpha_1 L_{ox}}{(1+A)^2} \\ \dfrac{A}{1+\frac{A}{\tau_2}} & \dfrac{M}{(1+\frac{A}{\tau_2})^2} - 1 \end{bmatrix} \tag{4.3}$$

4.2 Existence of Traveling Waves

Definition 4.2.1 *A traveling wave solution of system (4.1) is a particular solution that represents a front with constant velocity connecting two equilibria of system (4.2). It is expressed as:*

$$\begin{pmatrix} M(t,x) \\ A(t,x) \end{pmatrix} = W(x - ct)$$

where the constant c is the speed of the wave and

$$\lim_{x \to \pm\infty} W(x) = W_{\pm} \tag{4.4}$$

with W_+ and W_- being two equilibria of system (4.2).

Proposition 4.2.1 *System (4.2) is globally monotone, i.e the off-diagonal elements of its Jacobian are non negative.*

Proposition 4.2.2 *The existence of traveling wave solutions of reaction-diffusion systems is ensured in the monostable case and the bistable case due to the monotonicity of the system. The uniqueness of waves holds in the bistable case but not in the monostable case (see e.g. [22], Theorem 1.1 and Theorem 1.2, Chapter 3).*

Theorem 4.2.3 *In the bistable case, there exists a unique traveling wave solution connecting the stable equilibria E_0 (non inflammatory state) and E_1 (inflammatory state), i.e. a constant c and a vector valued function $W(x - ct)$ solution of the system (4.1) on the real line $]-\infty, \infty[$ and that satisfies Eq. (4.4) where $W_- = E_0$ and $W_+ = E_1$.*

Theorem 4.2.4 *In the monstable case, there exists a constant c^* such that $\forall c \in [c^*, \infty[$, there exists a traveling wave solution of velocity c connecting the unstable equilibrium E_0 to the stable one E_1, i.e. a vector valued function $W(x - ct)$, solution of the system (4.1) on the real line $]-\infty, \infty[$ and that satisfies Eq. (4.4) where $W_- = E_0$ and $W_+ = E_1$.*

4.3 Numerical Simulations

We implement and show the obtained results through numerical simulations to solve the system (4.1) on the 1D interval $]0, 1[$ equipped with its respective homogeneous Neumann boundary conditions.
We perform the simulations using COMSOL Multiphysics and we represent in appendix B the model report for the monostable case.

Monostable Case

The values of the parameters are $d_L = d_r = d_{L_{ox}} = d_M = d_A = 10^{-4}$, $\sigma_L = 1$, $s_L = 10$, $\lambda_L = 1$, $\sigma_r = 1$, $\lambda_r = 1$, $\lambda_{L_{ox}} = 1$, $\alpha_1 = 10$, $\beta_1 = 10$, $\lambda_M = 1$ and $\tau_2 = 1$.

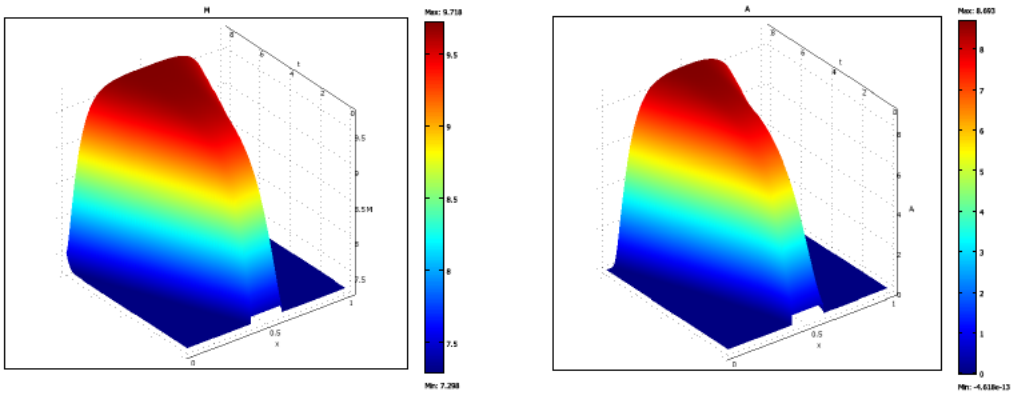

Figure 4.1: In the monostable case, we notice that even a small perturbation of the non-inflammatory state will lead to the propagation of a chronic inflammatory reaction.

Bistable Case

The values of the parameters are $d_L = d_r = d_{L_{ox}} = d_M = d_A = 10^{-4}$, $\sigma_L = 1$, $s_L = 0.001$, $\lambda_L = 1$, $\sigma_r = 1$, $\lambda_r = 1$, $\lambda_{L_{ox}} = 1$, $\alpha_1 = 100$, $\beta_1 = 15$, $\lambda_M = 1$ and $\tau_2 = 2$.

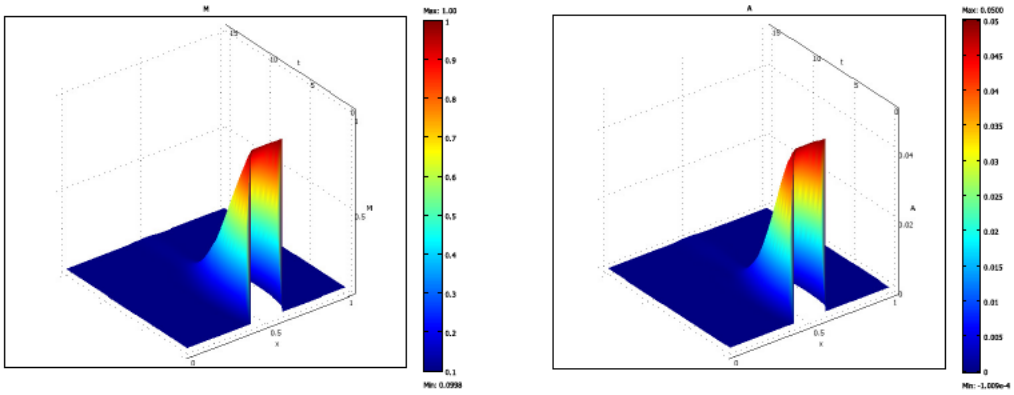

Figure 4.2: A small perturbation of the non-inflammatory state will not lead to the propagation of a chronic inflammatory reaction.

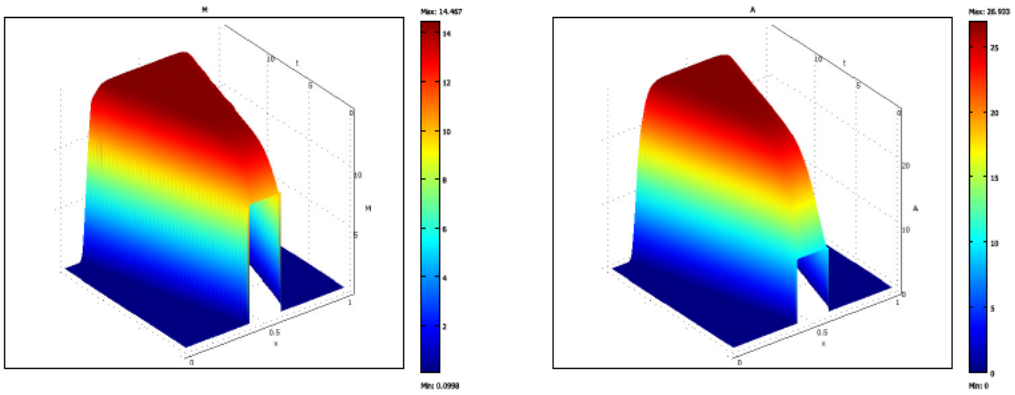

Figure 4.3: A large perturbation of the non-inflammatory state will lead to the propagation of a chronic inflammatory reaction.

Chapter 5

Two Dimensional Model

5.1 Model Description

We expand the study to the Two-Dimensional case, i.e by taking the domain representing the intima as a rectangle $\Omega_\varepsilon = [\,0, L\,] \times [\,0, \varepsilon]$. The difference is by considering the agents that involve the recruitment from the blood flow as boundary conditions, not as source terms.
The upper horizontal side of the rectangle (Boundary 3) is the boundary between the intima and the blood flow and the length of both vertical sides is ε (refer to Fig. (5.1)). We expect to observe the convergence towards the $1D$ case as $\varepsilon \longrightarrow 0$.
The $2D$ model is defined by:

$$\begin{cases} \dfrac{\partial L}{\partial t} = d_L \Delta L - s_L r L - \lambda_L L \\ \dfrac{\partial r}{\partial t} = d_r \Delta r + \sigma_r - s_L r L - \lambda_r r \\ \dfrac{\partial L_{ox}}{\partial t} = d_{L_{ox}} \Delta L_{ox} + s_L r L - \lambda_{L_{ox}} L_{ox} \\ \dfrac{\partial M}{\partial t} = d_M \Delta M - \lambda_M M \\ \dfrac{\partial A}{\partial t} = d_A \Delta A + \dfrac{\alpha_2 A M}{1 + \frac{A}{\tau_2}} - \lambda_A A \end{cases} \tag{5.1}$$

on the domain Ω_ε and $t \in [\,0, \infty[$.
Due to the small thickness of the intima relatively to the dimensions of the atherosclerotic lesion, the incoming flux of LDL particles and immune cells decreases proportionally to the width of the domain. For that reason, the parameter ε appears in the boundary conditions.
On the lower and both vertical sides (boundaries 1, 2 and 4), we impose homogeneous Neumann boundary conditions for the five unknowns. Besides, boundary conditions on the upper side (Boundary 3) for $x \in [\,0, L]$ are:

$$\frac{\partial L}{\partial y}(x, \varepsilon) = \frac{\varepsilon}{d_L} \sigma_L, \;\; \frac{\partial M}{\partial y}(x, \varepsilon) = \frac{\varepsilon}{d_M} \left(\frac{\alpha_1 L_{ox} + \beta_1 A}{1 + \frac{A}{\tau_1}} \right)$$

$$\frac{\partial r}{\partial y}(x,\varepsilon) = \frac{\partial L_{ox}}{\partial y}(x,\varepsilon) = \frac{\partial A}{\partial y}(x,\varepsilon) = 0$$

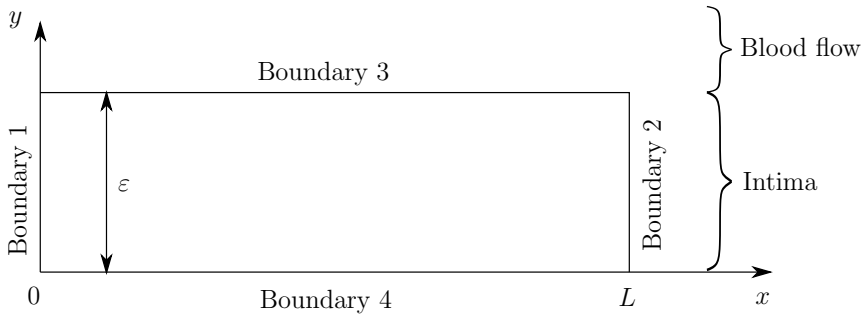

Figure 5.1: Geometry of the rectangular domain.

5.2 Boundary Conditions Scaling

We consider the following change of variable $z = y/\varepsilon$ and we set $\tilde{M}(t,x,z) = M(t,x,y)$ in order to explain the scaled boundary condition for M. For the ease of notation, we set $F = F(L_{ox}, A) = \dfrac{\alpha_1 L_{ox} + \beta_1 A}{1 + \frac{A}{\tau_1}}$.

We obtain:

$$\frac{\partial \tilde{M}}{\partial t} = d_M \frac{\partial^2 \tilde{M}}{\partial x^2} + \frac{d_M}{\varepsilon^2}\frac{\partial^2 \tilde{M}}{\partial z^2} - \lambda_M \tilde{M} \tag{5.2}$$

for $(x,z) \in \Omega = [\,0,L\,] \times [\,0,1\,]$ and $t \in [\,0,\infty[\,$, equipped with homogeneous Neumann boundary conditions on the lower horizontal side and on the both vertical sides (Boundaries 1,2 and 4 in Fig. (5.1)) and with

$$\frac{\partial \tilde{M}}{\partial z}(x,1) = \frac{F}{d_M}\varepsilon^2 \tag{5.3}$$

for $x \in [\,0,L\,]$ on the upper horizontal side (Boundary 3).
We consider the formal expansion of $\tilde{M}$ given by Eq. (5.4) and insert it in Eqs. (5.2) and (5.3).

$$\tilde{M}(t,x,z) = M_0(t,x,z) + \varepsilon M_1(t,x,z) + \varepsilon^2 M_2(t,x,z) + \cdots \tag{5.4}$$

- We identify and collect the coefficients of ε^{-2} in Eq. (5.2) and using the boundary conditions for the upper and lower horizontal sides, we get:

$$\begin{cases} \dfrac{\partial^2 M_0}{\partial z^2} = 0 \ \text{ on the domain } \Omega \\ \dfrac{\partial M_0}{\partial z}(x,0) = \dfrac{\partial M_0}{\partial z}(x,1) = 0 \ \text{ for } x \in [\,0,L\,] \end{cases}$$

  From that, we notice that M_0 is independent of z

- Identifying and collecting the coefficients of ε^0 in Eq. (5.2) gives:

$$\frac{\partial M_0}{\partial t} = d_M \frac{\partial^2 M_0}{\partial x^2} + d_M \frac{\partial^2 M_2}{\partial z^2} - \lambda_M M_0$$

Integrating both sides of the last equation with respect to z from 0 to 1 and knowing that M_0 is independent of z yields:

$$\frac{\partial M_0}{\partial t} = d_M \frac{\partial^2 M_0}{\partial x^2} + d_M \frac{\partial M_2}{\partial z}(x,1) - d_M \frac{\partial M_2}{\partial z}(x,0) - \lambda_M M_0$$

- Finally identifying and collecting the coefficients of ε^2 in Eq. (5.3) and using the boundary conditions for the lower horizontal side leads to:

$$\begin{cases} \dfrac{\partial M_2}{\partial z}(x,1) = \dfrac{F}{d_M} \\ \dfrac{\partial M_2}{\partial z}(x,0) = 0 \end{cases}$$

With this, one can obtain the $1D$ equation:

$$\frac{\partial M_0}{\partial t} = d_M \frac{\partial^2 M_0}{\partial x^2} + F - \lambda_M M_0$$

Therefore, the solution of the $2D$ model tends formally towards that of the $1D$ model when $\varepsilon \longrightarrow 0$.

Remark 5.2.1 *The same reasoning is applicable for the variable L to show the convergence towards the $1D$ model and to explain the scaled boundary condition.*

5.3 Reduction of the System

For the same reason discussed earlier in Section 4.1, we reduce the $2D$ model into:

$$\begin{cases} \dfrac{\partial M}{\partial t} = d_M \Delta M - \lambda_M M \\ \dfrac{\partial A}{\partial t} = d_A \Delta A + \dfrac{\alpha_2 A M}{1 + \frac{A}{\tau_2}} - \lambda_A A \end{cases} \tag{5.5}$$

Existence of traveling waves and numerical simulations are performed based on the reduced system (5.5).

5.4 Numerical Simulations

Convergence to the $1D$ model is shown now through numerical simulations using COMSOL Multiphysics.
In both monostable and bistable cases, we take the same values of the parameters as in Chap.4 and we observe the same qualitative behavior as for the $1D$ case assuming that the domain is thin enough, i.e for $\varepsilon \longrightarrow 0$. For that, we consider the $2D$ domain $\Omega_\varepsilon = [\,0,1\,] \times [\,0,\varepsilon\,]$ with $\varepsilon = 10^{-3}$.

Monostable Case

In the monostable case, one can refer to reference [14] for the detailed proof of existence of traveling waves. Results are shown numerically and we observe the same behavior as in the $1D$ case for ε small enough.
Fig. (5.2) illustrates such a result.

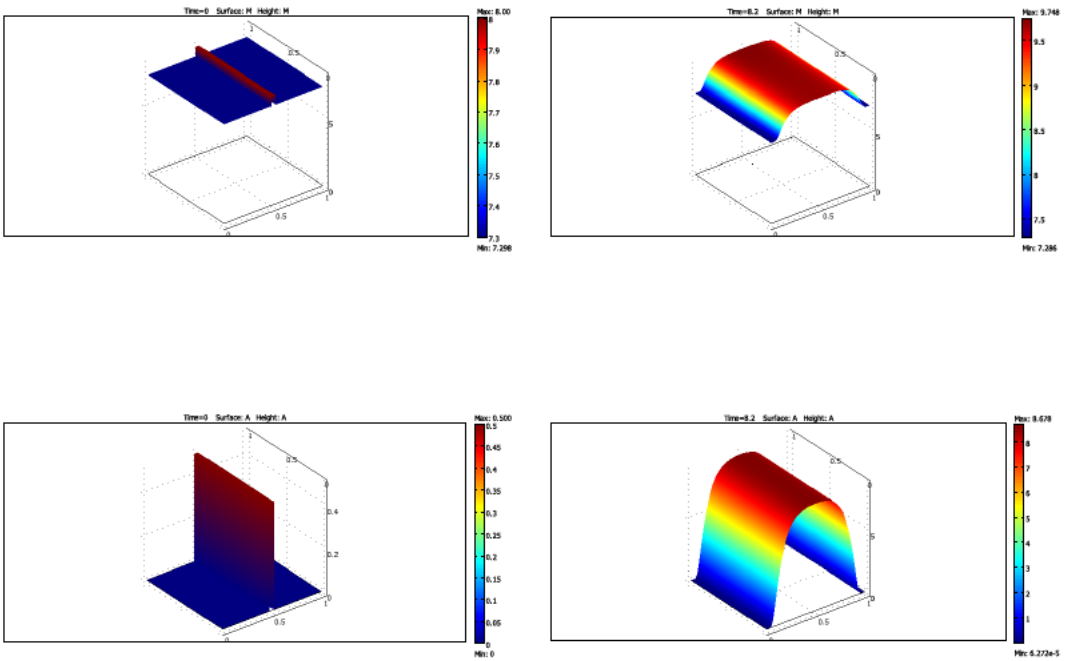

Figure 5.2: In the monostable case, we notice that even a small perturbation of the non-inflammatory state will lead to the set up of a chronic inflammatory reaction. Moreover, the solution very weakly depends on y.
Left: Solution at $t = 0$. Right: Solution at $t = 8.2$.

Bistable Case

Existence of solution of traveling wave type in the bistable case is only performed numerically. The same threshold effect occurs as in the $1D$ case: a small perturbation of the non-inflammatory state does not lead to the propagation of a chronic inflammatory reaction, whereas a large perturbation does. Refer to Figs. (5.3) and (5.4) for the illustration of the result.

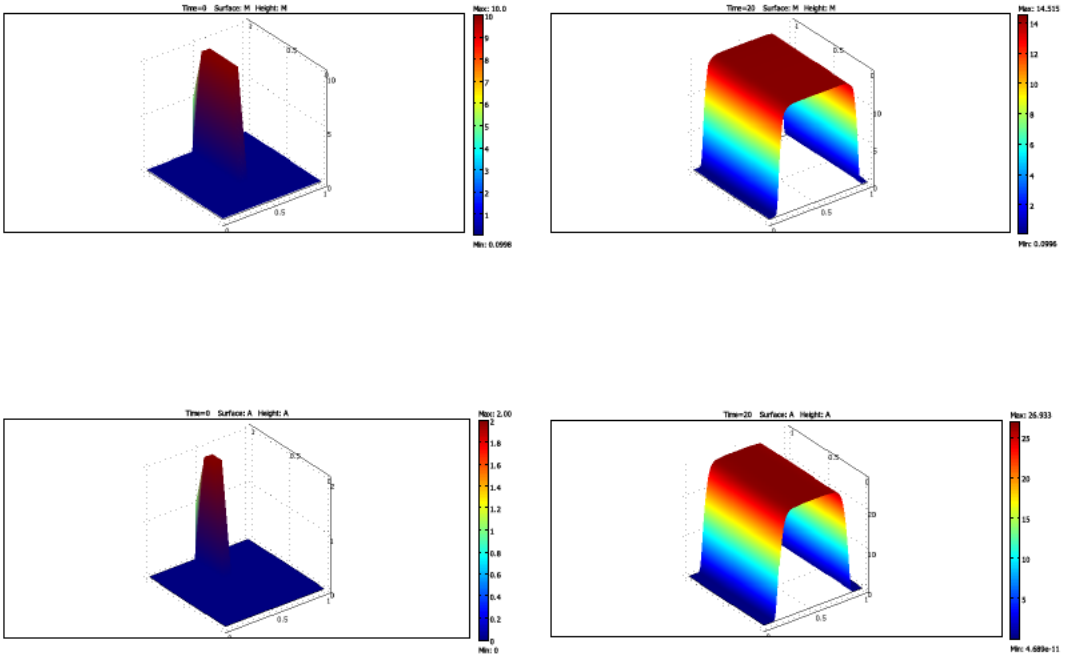

Figure 5.3: We observe that the solution weakly depends on y. In addition, a large perturbation of the noninflammatory state will lead to the set of an inflammatory reaction.
Left: Solution at $t = 0$. Right: Solution at $t = 20$.

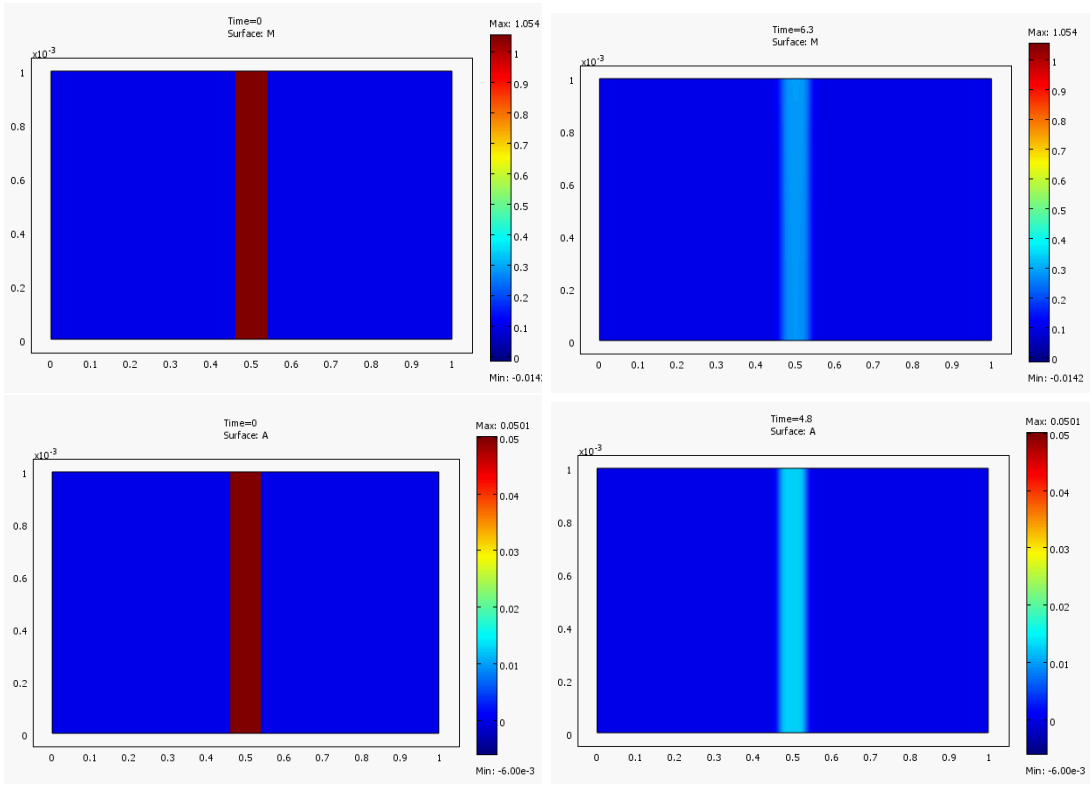

Figure 5.4: Similarly, the solution weakly depends on y. Besides, a small perturbation of the noninflammatory state will not lead to the set up of a chronic inflammatory reaction.
Left: Initial condition. Right: Subsequent time.

Chapter 6

Conclusion

In this thesis, a $1D$ and a $2D$ mathematical models for the early stages of atherosclerosis are developed. Results have shown an enhancement and approval of those achieved in [1].
Five key-role players are considered: LDL, free radicals, ox-LDL, macrophages and cytokines. Three new agents are able to render the model more realistic and fits what really occurs in human's intima.
In fact, the results show that the inflammatory process highly depends on the initial quantity of ox-LDL in the intima, but this initial quantity is mainly affected by LDL particles and free radicals. This result has the potential to shed light on encouraging people to reduce the amount of low density lipoproteins and to boost the amount of antioxidant species.
The existence of a traveling wave solution is validated theoretically and numerically. Its goal is to describe the set up of the inflammatory reaction as a traveling wave inside the intima. Moreover, the convergence of the $2D$ model into the $1D$ model is performed in the thin domain.

This research can be expanded by considering more key-role players: the ones that trigger the inflammation and the ones that attenuates the process. For example, one can consider the role of high density lipoproteins (HDL). HDL particles act as free radicals sponges, they are prone to oxidation processes as LDL. This is beneficial by the fact that ox-HDL does not contribute to the atherosclerotic process whereas ox-LDL actually instigates it. [16]
Besides, the role of the permeability of the endothelium would be very important. Permeability can be considered as the first initiator of the inflammation, for that it would be interesting if one studies its effect on the inflammatory process.

Bibliography

[1] N. El Khatib, S. Génieys, B. Kazmierczak, and V. Volpert. Mathematical modelling of atherosclerosis as an inflammatory disease. *Mathematical Modelling of Natural Phenomena*, 2:126–141, 01 2007.

[2] Alain Tedgui and Ziad Mallat. Cytokines in atherosclerosis: Pathogenic and regulatory pathways. *Physiological reviews*, 86:515–81, 05 2006.

[3] Gregory Roth, Kalkidan Abate, Solomon Abay, Abbafati Cristiana, Nooshin Abbasi, Hedayat Abbastabar, Foad Abd-Allah, Jemal Ebro, Ahmed Abdelalim, Ibrahim Abdollahpour, Rizwan Suliankatchi, Haftom Abebe, Molla Abebe, Zegeye Abebe, Ayenew Abejie, Semaw Abera, Olifan Zewdie, and Haftom Niguse. Global, regional, and national age-sex-specific mortality for 282 causes of death in 195 countries and territories, 1980–2017: a systematic analysis for the global burden of disease study 2017. *The Lancet*, 392:1736–1788, 11 2018.

[4] Vladimir Bezyaev, Nail Sadekov, and Vitaly Volpert. A model of chronic inflammation in atherosclerosis. *ITM Web of Conferences*, 31:04002, 01 2020.

[5] Number of deaths by cause, world, 2017. `https://ourworldindata.org/grapher/annual-number-of-deaths-by-cause?country=~OWID_WRL`.

[6] C.A Cobbold, J.A Sherratt, and S.R.J Maxwell. Lipoprotein oxidation and its significance for atherosclerosis: a mathematical approach. *Bulletin of Mathematical Biology*, 64(1):65 – 95, 2002.

[7] An overview of atherosclerosis. `https://www.verywellhealth.com/what-is-atherosclerosis-1745908`. Accessed: 2020-01-04.

[8] Sadip Pant, Abhishek Deshmukh, Guru Gurumurthy, Naga Pothineni, Thomas Watts, Francesco Romeo, and Jawahar Mehta. Inflammation and atherosclerosis–revisited. *Journal of cardiovascular pharmacology and therapeutics*, 19, 10 2013.

[9] Yuri V. Bobryshev. Monocyte recruitment and foam cell formation in atherosclerosis. *Micron*, 37(3):208 – 222, 2006.

[10] E. Leiva, S. Wehinger, L. Guzmán, and R. Orrego. Role of oxidized ldl in atherosclerosis. In Sekar Ashok Kumar, editor, *Hypercholesterolemia*, chapter 3. IntechOpen, Rijeka, 2015.

[11] Md. Hamidul Islam. *Mathematical Modelling of the Inflammatory Response in Coronary Artery Disease*. PhD thesis, Griffith University, 2017.

[12] Joe Moss and Dipak Ramji. Cytokines: Roles in atherosclerosis disease progression and potential therapeutic targets. *Future Medicinal Chemistry*, 8, 06 2016.

[13] M. Abdulsalam and J. Feng. Distinguish the stable and unstable plaques based on arterial waveform analysis. *Procedia Structural Integrity*, 15:2 – 7, 2019. International Conference on Stents: Materials, Mechanics and Manufacturing ICS3M 2019.

[14] Nader EL Khatib, Stéphane Génieys, and Bogdan Kazmierczak. Reaction-diffusion model of atherosclerosis development. *Journal of mathematical biology*, 65:349–74, 08 2011.

[15] Anna Ougrinovskaia, Rosemary Thompson, and Mary Myerscough. An ode model of early stages of atherosclerosis: Mechanisms of the inflammatory response. *Bulletin of mathematical biology*, 72:1534–61, 05 2010.

[16] Cameron Mckay, Sean Mckee, Nigel Mottram, Tony Mulholl, Stephen Wilson, Simon Kennedy, and Roger Wadsworth. Towards a model of atherosclerosis.

[17] MAK Bulelzai. *Mathematical models for atherosclerotic plaque evolution*. PhD thesis, Delft University of Technology, 2013.

[18] Jorge Tiago, Telma Silva, Adélia Sequeira, and Rafael Santos. Mathematical modeling of atherosclerotic plaque formation coupled with a non-newtonian model of blood flow. *Conference Papers in Mathematics*, 2013, 07 2013.

[19] P. Thon Moritz, R. Myerscough Mary, and W. Gee Michael. A spatially resolved and quantitative model of early atherosclerosis. *Journal of mathematical biology*, 81:4022–4068, 2019.

[20] Wanwarat Anlamlert, Yongwimon Lenbury, and Jonathan Bell. Modeling fibrous cap formation in atherosclerotic plaque development: stability and oscillatory behavior. *Advances in Difference Equations*, 2017, 07 2017.

[21] Jorge Tiago, Rafael Santos, Adélia Sequeira, and Telma Silva. Existence, uniqueness, stability and asymptotic behavior of solutions for a mathematical model of atherosclerosis. *Discrete and Continuous Dynamical Systems - Series S*, 9:343–362, 12 2015.

[22] A. I. Volpert. *Traveling Wave Solutions of Parabolic Systems: Translations of Mathematical Monographs*, volume 140. American Mathematical Society, 1994.

Appendix A

Computations

Non-dimensionlization of the system of Eqs. (3.2)

Let $L = \lambda_A \tilde{L};\ r = \lambda_A \tilde{r};\ L_{ox} = \lambda_A \tilde{L}_{ox};\ M = \dfrac{\lambda_A}{\alpha_2}\tilde{M};\ A = \tau_1 \tilde{A};\ t = \dfrac{1}{\lambda_A}\tilde{t}$
Using these transformations, we obtain:

$$\begin{cases} \dfrac{d\tilde{L}}{d\tilde{t}} = \dfrac{\sigma_L}{\lambda_A^2} - s_L \tilde{r}\tilde{L} - \dfrac{\lambda_L}{\lambda_A}\tilde{L} \\ \dfrac{d\tilde{r}}{d\tilde{t}} = \dfrac{\sigma_r}{\lambda_A^2} - s_L \tilde{r}\tilde{L} - \dfrac{\lambda_r}{\lambda_A}\tilde{r} \\ \dfrac{d\tilde{L}_{ox}}{d\tilde{t}} = s_L \tilde{r}\tilde{L} - \dfrac{\lambda_{L_{ox}}}{\lambda_A}\tilde{L_{ox}} \\ \dfrac{d\tilde{M}}{d\tilde{t}} = \dfrac{\frac{\alpha_1\alpha_2}{\lambda_A}\tilde{L}_{ox} + \frac{\beta_1\tau_1\alpha_2}{\lambda_A^2}\tilde{A}}{1+\tilde{A}} - \dfrac{\lambda_M}{\lambda_A}\tilde{M} \\ \dfrac{d\tilde{A}}{d\tilde{t}} = \dfrac{\tilde{A}\tilde{M}}{1+\frac{\tau_1}{\tau_2}\tilde{A}} - \tilde{A} \end{cases} \tag{A.1}$$

We denote by:
$\tilde{\sigma}_L = \dfrac{\sigma_L}{\lambda_A^2};\ \tilde{\lambda}_L = \dfrac{\lambda_L}{\lambda_A};\ \tilde{\sigma}_r = \dfrac{\sigma_r}{\lambda_A^2};\ \tilde{\lambda_r} = \dfrac{\lambda_r}{\lambda_A};\ \tilde{\lambda}_{L_{ox}} = \dfrac{\lambda_{L_{ox}}}{\lambda_A};\ \tilde{\alpha}_1 = \dfrac{\alpha_2\alpha_1}{\lambda_A};\ \tilde{\beta}_1 = \dfrac{\beta_1\tau_1\alpha_2}{\lambda_A^2};$
$\tilde{\lambda}_M = \dfrac{\lambda_M}{\lambda_A};\ \tilde{\tau}_2 = \dfrac{\tau_2}{\tau_1}$
We replace these notations in the system (A.1), we drop the tildes to avoid any abuse of notation and then obtain the dimensionless system of equations (3.3).

Detailed Computations for the Three Cases presented in Part (3.2.2)

Our goal is to determine all possible non-negative intersections of g_1 with g_2 i.e the solutions of

$$g(A) = A^2 + \left(\tau_2 + 1 - \frac{\beta_1\tau_2}{\lambda_M}\right)A + \tau_2\left(1 - \frac{\alpha_1\gamma}{\lambda_M\lambda_{L_{ox}}}\right) = 0 \tag{A.2}$$

The discriminant of Eq.(A.2) is given by:

$$\Delta_{g(A)} = \left(1 - \frac{\beta_1}{\lambda_M}\right)^2 \tau_2^2 + 2\left(\frac{2\alpha_1\gamma}{\lambda_M\lambda_{L_{ox}}} - \frac{\beta_1}{\lambda_M} - 1\right)\tau_2 + 1$$

We introduce as well the product p and the sum s of the roots of Eq.(A.2): $p = \tau_2\left(1 - \frac{\alpha_1\gamma}{\lambda_M\lambda_{L_{ox}}}\right)$ and $s = \frac{\beta_1\tau_2}{\lambda_M} - \tau_2 - 1$
We observe three different cases:

(i) If $\frac{\alpha_1\gamma}{\lambda_M\lambda_{L_{ox}}} > 1$ then $p < 0$ and we obtain only one positive solution E_1 for Eq.(A.2)

(ii) If

$$\frac{\alpha_1\gamma}{\lambda_M\lambda_{L_{ox}}} < 1 < \frac{\beta_1}{\lambda_M} \tag{A.3}$$

Then $p > 0$
We first consider $\Delta_{g(A)}$ as a second order polynomial with respect to τ_2 and we study its sign accordingly. Its reduced discriminant is:

$$\Delta'_{\tau_2} = 4\left(\frac{\alpha_1\gamma}{\lambda_M\lambda_{L_{ox}}} - 1\right)\left(\frac{\alpha_1\gamma}{\lambda_M\lambda_{L_{ox}}} - \frac{\beta_1}{\lambda_M}\right)$$

We notice that $\Delta'_{\tau_2} > 0$ due to condition (A.3).
The roots τ_- and τ_+ of $\Delta_{g(A)}$ are:

$$\tau_- = \frac{1}{(1 - \frac{\beta_1}{\lambda_M})^2}\left(\sqrt{1 - \frac{\alpha_1\gamma}{\lambda_M\lambda_{L_{ox}}}} - \sqrt{\frac{\beta_1}{\lambda_M} - \frac{\alpha_1\gamma}{\lambda_M\lambda_{L_{ox}}}}\right)^2$$

$$\tau_+ = \frac{1}{(1 - \frac{\beta_1}{\lambda_M})^2}\left(\sqrt{1 - \frac{\alpha_1\gamma}{\lambda_M\lambda_{L_{ox}}}} + \sqrt{\frac{\beta_1}{\lambda_M} - \frac{\alpha_1\gamma}{\lambda_M\lambda_{L_{ox}}}}\right)^2$$

Based on condition (A.3), we note that:

$$\tau_- < \frac{1}{\frac{\beta_1}{\lambda_M} - 1} < \tau_+ \tag{A.4}$$

We conclude that:

- If $0 < \tau_2 \leq \tau_-$ then $\Delta_{g(A)} \geq 0$. But $s < 0$ so Eq.(A.2) has two negative solutions.
- If $\tau_- < \tau_2 < \tau_+$ then $\Delta_{g(A)} < 0$, thus Eq.(A.2) has no real solution.
- If $\tau_+ = \tau_2$ then $\Delta_{g(A)} = 0$, consequently Eq.(A.2) has a double positive root E_1.
- If $\tau_+ < \tau_2$ then $\Delta_{g(A)} > 0$. Moreover $s > 0$ according to inequality (A.4). Hence Eq.(A.2) admits two positive solutions E_u and E_1.

(iii) $\frac{\alpha_1\gamma}{\lambda_M\lambda_{L_{ox}}} < \frac{\beta_1}{\lambda_M} \leq 1$ then $p > 0$ and $s < 0$, thus Eq.(A.2) admits two negative solutions.

(iv) $\frac{\alpha_1\gamma}{\lambda_M\lambda_{L_{ox}}} = 1 \geq \frac{\beta_1}{\lambda_M}$ then $p = 0$ and $s < 0$, hence Eq.(A.2) has a negative solution and a zero solution that is combined with E_0.

(v) $\frac{\alpha_1\gamma}{\lambda_M\lambda_{L_{ox}}} = 1 < \frac{\beta_1}{\lambda_M}$ then $p = 0$
In addition, $\Delta_{g(A)}$ considered as a second order polynomial with respect to τ_2 has a double root $\tau^* = \frac{1}{\frac{\beta_1}{\lambda_M} - 1}$
We conclude that:

- If $0 < \tau_2 < \tau^*$, then $\Delta_{g(A)} > 0$ and $s < 0$, hence Eq.(A.2) has a negative solution and a zero solution that is combined with E_0.
- If $\tau_2 = \tau^*$, then $\Delta_{g(A)} = 0$ and $s = 0$, therefore Eq.(A.2) admits a double root that is combined with E_0.
- $\tau_2 > \tau^*$, then $\Delta_{g(A)} > 0$ and $s > 0$, thus Eq.(A.2) has a positive solution E_1 and a zero solution that is combined with E_0.

Effect of σ_L and σ_r on γ

$\gamma = \sigma_r - \lambda_r r^* = \sigma_r - \frac{s_L\sigma_r - s_L\sigma_L - \lambda_r\lambda_L + \sqrt{\Delta}}{2s_L}$
with $\Delta = s_L\sigma_L + \lambda_r\lambda_L - s_L\sigma_r)^2 + 4s_L\lambda_r\sigma_r\lambda_L$

The sign of $\frac{\partial\gamma}{\partial\sigma_r}$ and $\frac{\partial\gamma}{\partial\sigma_L}$ helps in understanding how γ is affected by the sources σ_L and σ_r.

- $\frac{\partial\gamma}{\partial\sigma_r} = \frac{1}{2} - \frac{1}{2}\left(\frac{-s_L\sigma_r - \lambda_r\lambda_L + s_L\sigma_L}{\sqrt{\Delta}}\right) > 0$
- $\frac{\partial\gamma}{\partial\sigma_L} = \frac{1}{2} - \frac{1}{2}\left(\frac{-s_L\sigma_r + \lambda_r\lambda_L + s_L\sigma_L}{\sqrt{\Delta}}\right) > 0$

Hence γ is large when both σ_L and σ_r are large.

Appendix B

Simulations

Matlab Code

```
% This matlab code enables us to plot the curves g1 & g2 and all the
% equilibrium points that exist, it shows whether these points are stable
% or not.

format short
syms x y

sigmaL=1;lambdaL=1; sL=1; sigmar=40; lambdar=1;  alpha1=20; beta1=4;
lambdaM=3;tau2=0.5;lambdaLox=10;alpha2=1; tau1=1; lambdaA=1; % parameters for
    case1

% sigmaL=1;lambdaL=1; sL=10; sigmar=1; lambdar=1;  alpha1=10; beta1=10;
% lambdaM=1;tau2=1;lambdaLox=1;alpha2=1; tau1=1; lambdaA=1; % parameters for
    case2

% sigmaL=1;lambdaL=1; sL=0.001; sigmar=1; lambdar=1;  alpha1=100; beta1=4;
% lambdaM=1;tau2=1;lambdaLox=1;alpha2=1; tau1=1; lambdaA=1; %parameters for
    case3

delta=(sL*sigmaL+lambdar*lambdaL-sL*sigmar)^2+4*sL*lambdar*sigmar*lambdaL;
r0=(sL*sigmar-sL*sigmaL-lambdar*lambdaL+sqrt(delta))/(2*sL*lambdar);
L0=(sigmaL-sigmar+lambdar*r0)/(lambdaL);
Lox0=(sL*r0*L0)/lambdaLox;
M0=(alpha1*Lox0)/(lambdaM);
A0=0;
E0 = [L0,r0,Lox0,M0,A0]; %coordinates of E0
g1 = (1/lambdaM)*((alpha1*Lox0+beta1*x)/(1+x/tau1));
g2 = (lambdaA/alpha2)*(1+x/tau2);

fplot(g2,'LineWidth',1.5,'color',[0.1  0.3  0.5]);hold on
fplot(g1,'LineWidth',1.5,'color',[0.8  0.1  0]);hold on

labels = {'$E_0$'};
plot(A0,M0,'.','color','black','MarkerSize',20)
text(A0,M0,labels,'VerticalAlignment','bottom','HorizontalAlignment','Right','
    interpreter','latex','FontSize',15)
hold on

a = 1/(tau1*tau2) ;
b = (1/tau1 + 1/tau2 - (beta1*alpha2)/(lambdaA*lambdaM));
c = (1-(alpha1*alpha2*(sL*r0*L0))/(lambdaA*lambdaM*lambdaLox));

Q=[a b c];
r=roots(Q);
[j,g]=size(r);
K=0;
 for i=1:j
      if r(i)>0 && imag(r(i))==0
        K=K+1;
     end
```

```
 end

 if K>0
 AA=zeros(K,1);
 MM=zeros(K,1);
 k1=0;
for i=1:j
    if r(i)>0 && imag(r(i))==0
        k1=k1+1;
        AA(k1)=r(i);
        MM(k1)=1+(AA(k1)/tau2);
    end
end
INTERSECTION = [MM(:),AA(:)];
else
     fprintf('No intersections between in the plane M=1+A/tau2')
end

if K>0
    [M,N]=size(INTERSECTION);

if M == 1
    M1 = INTERSECTION(1,1);
    A1 = INTERSECTION(1,2);
    E1=[L0, r0, Lox0, M1,A1];
labels = {'$E_1$'};
plot(A1,M1,'.','color','black','MarkerSize',20);
text(A1,M1,labels,'VerticalAlignment','top','HorizontalAlignment','Left','
    interpreter','latex','FontSize',15)
hold on

elseif M == 2
    M1= INTERSECTION (1,1);
    A1= INTERSECTION (1,2);

    M2= INTERSECTION (2,1);
    A2= INTERSECTION (2,2);
    E1=[L0, r0, Lox0, M1,A1];
    Eu=[L0, r0, Lox0, M2,A2];

labels = {'$E_1$'};
plot(A1,M1,'.','color','black','MarkerSize',20);
text(A1,M1,labels,'VerticalAlignment','bottom','HorizontalAlignment','Right','
    interpreter','latex','FontSize',15)
hold on

labels = {'$E_u$'};
plot(A2,M2,'.','color','black','MarkerSize',20);
text(A2,M2,labels,'VerticalAlignment','bottom','HorizontalAlignment','Right','
    interpreter','latex','FontSize',15)
hold on
end
end

%choice of starting points for case1
q=[ 0.2,0.2,0.01,0.5,0.5 ; 1,1,0.01,0.6,0.9 ; 0.7,0.6,0.01,2,1.6 ; 0.8,2,1,0.8,1
     ; 2,2,0.1,1.1,1.3 ; 2,1.6,0.2,2,0.7 ; 2,2,0.1,2.1,1.2 ; 1,2,0.1,1.5,1.7];

%choice of starting points for case2
% q=[ 0.5,0.5,0.01,5.6,2 ; 0.6,0.7,0.01,8,5 ; 0.8,0.8,0.01,11,7 ;
    0.1,0.1,1,11,5; 2,2,0.1,7,1 ; 2.5,2,0.2,6,0.3 ; 2,2,0.1,8.5,0.2 ;
    1,1,0.1,11.5,3 ; 0.1,0.1,0.1,10.5,2];

%choice of starting points for case3
% q=[0.8,0.8,0.01,0.3,0.5 ; 0.8,0.8,0.01,0.75,0.1 ; 0.8,0.8,0.01,0.5,0.3 ;
    0.8,0.8,0.01,1.5,0.2 ; 1.2,1.2,0.01,1,0.5 ; 1.2,1.2,0.2,2.8,3 ;
    2,2,0.1,1.75,1.25 ; 2,2,0.1,1.5,1 ; 2,2,0.2,3.2,2.5];

niter=100; deltat=0.01;
[m,n]=size(q);
for i=1:m
    L_0=q(i,1);
    r_0=q(i,2);
```

```
    Lox_0=q(i,3);
    M_0=q(i,4);
    A_0=q(i,5);

    P=zeros(niter/deltat+1,2);
    P(1,:)=[A_0 M_0];
    j=2;
    for t=0:deltat:niter

        LLL = (sigmaL - sL*r_0*L_0 - lambdaL*L_0)*deltat + L_0;
        rrr = (sigmar - sL*r_0*L_0 - lambdar*r_0)*deltat + r_0;
        LoxLox=Lox_0+deltat*(sL*r_0*L_0 - lambdaLox*Lox_0);
        MMM=M_0+deltat*((alpha1*Lox_0 + beta1*A_0)/(1+(A_0/tau1)) - lambdaM*M_0)
            ;
        AAA=A_0+deltat*((alpha2*A_0*M_0)/(1+(A_0/tau2)) - lambdaA*A_0);

        P(j,:)=[AAA MMM];
        j=j+1;
        L_0=LLL; r_0=rrr; Lox_0=LoxLox; M_0=MMM; A_0=AAA;
    end
    plot(P(:,1),P(:,2),'k-','LineWidth',0.5,'color',[0.2 0.2 0.2]);
    hold on

xlim([-0.6 ,2]);ylim([0.4 ,2.3]); %axes limiting for case 1
% xlim([-0.6 ,10]);ylim([5 ,12]); %axes limiting for case 2
% xlim([-1 ,4]);ylim([-0.2 ,5.1]); %axes limiting for case 3
end

grid off
xlabel('$A$','fontsize',15,'interpreter','latex')
ylabel('$M$','fontsize',15,'interpreter','latex')
leg1 = legend('$g_2$','$g_1$');
set(leg1,'Interpreter','latex');
set(leg1,'FontSize',15);
```

COMSOL Model Report

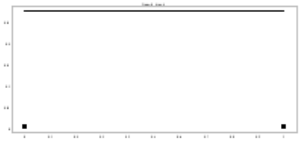

1. Table of Contents

- Title - COMSOL Model Report
- Table of Contents
- Model Properties
- Constants
- Geometry
- Geom1
- Solver Settings
- Postprocessing

2. Model Properties

Property	**Value**
Model name	
Author	
Company	
Department	
Reference	
URL	
Saved date	Apr 27, 2021 9:08:28 PM
Creation date	Apr 27, 2021 7:27:56 PM
COMSOL version	COMSOL 3.5.0.603

File name: C:\Users\Lenovo\Desktop\AtheroTrial.mph
Application modes and modules used in this model:
- Geom1 (1D)
  - PDE, Coefficient Form

3. Constants

Name	Expression	Value	Description
sigmaL	1	1	
sL	10	10	
lambdaL	1	1	
sigmar	1	1	
lambdar	1	1	
lambdaLox	1	1	
alpha1	10	10	
beta1	10	10	
lambdaM	1	1	
tau2	1	1	
E0L	0.2702	0.2702	
E0r	0.2702	0.2702	
E0Lox	0.7298	0.7298	
E0M	7.2984	7.2984	
E0A	0	0	
E1L	0.2702	0.2702	
E1r	0.2702	0.2702	
E1Lox	0.7298	0.7298	
E1M	9.7221	9.7221	
E1A	8.7221	8.7221	

4. Geometry

Number of geometries: 1

4.1. Geom1

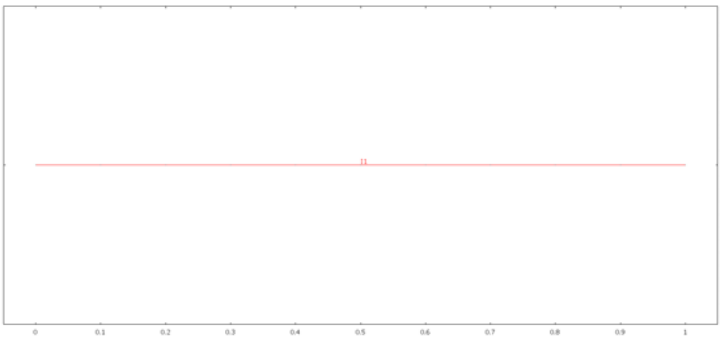

4.1.1. Boundary mode

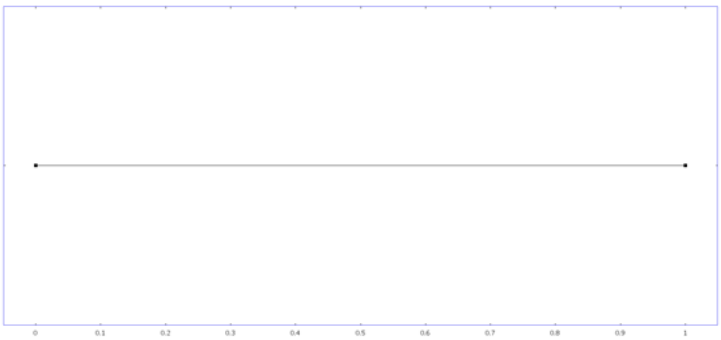

4.1.2. Subdomain mode

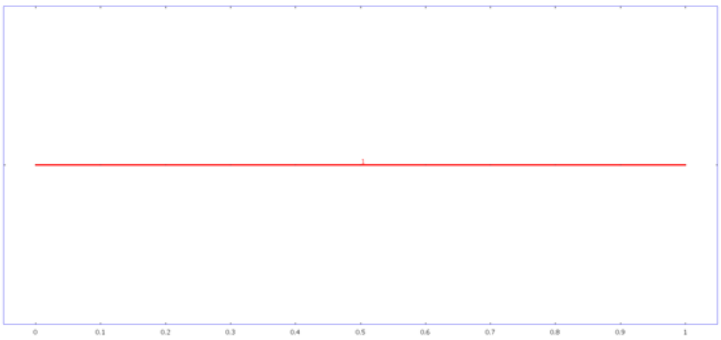

5. Geom1

Space dimensions: 1D
Independent variables: x, y, z

5.1. Mesh

5.1.1. Mesh Statistics

Number of degrees of freedom	76805
Number of mesh points	7681
Number of elements	7680
Number of boundary elements	2
Element length ratio	1

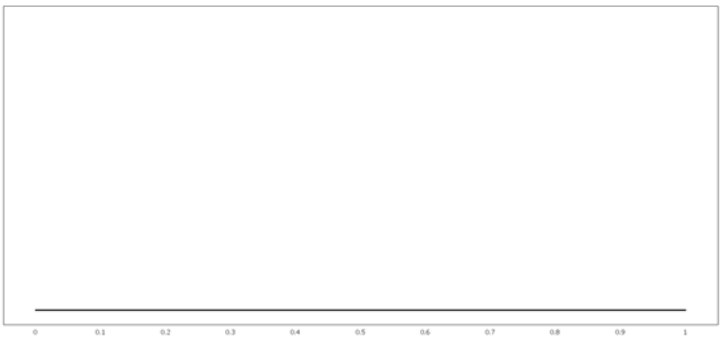

5.2. Application Mode: PDE, Coefficient Form (AtheroTrial)

Application mode type: PDE, Coefficient Form
Application mode name: AtheroTrial

5.2.1. Application Mode Properties

Property	**Value**
Default element type	Lagrange - Quadratic
Wave extension	Off
Frame	Frame (ref)
Weak constraints	Off

5.2.2. Variables

Dependent variables: L, r, Lox, M, A, L_t, r_t, Lox_t, M_t, A_t
Shape functions: shlag(2,'L'), shlag(2,'r'), shlag(2,'Lox'), shlag(2,'M'), shlag(2,'A')
Interior boundaries not active

5.2.3. Boundary Settings

Point	1-2
type	**Neumann boundary condition**

5.2.4. Subdomain Settings

Subdomain	1
Diffusion coefficient (c)	**{0.0001,0,0,0,0; 0,0.0001,0,0,0; 0,0,0.0001,0,0;**

Source term (f)	**{sigma1*L*r-lambdar*r;sigma1*L*r-lambdaL*L;sigmar-sL*r*L-lambdar*r;sL*r*L-lambdaLox*Lox;(alpha1*Lox+beta1*A)/(1+A)-lambdaM*M;(A*M)/(1+A/tau2)-A}**
Subdomain initial value	1
L	(sign(0.6-x)+sign(x-0.4))*0.5*(0.3-E0L)+E0L
r	(sign(0.6-x)+sign(x-0.4))*0.5*(0.3-E0r)+E0r
Lox	(sign(0.6-x)+sign(x-0.4))*0.5*(0.8-E0Lox)+E0Lox
M	(sign(0.6-x)+sign(x-0.4))*0.5*(7.4-E0M)+E0M
A	(sign(0.6-x)+sign(x-0.4))*0.5*(0.5-E0A)+E0A

6. Solver Settings

Solve using a script: off

Auto select solver	On
Solver	Time dependent
Solution form	Automatic
Symmetric	auto
Adaptive mesh refinement	Off
Optimization/Sensitivity	Off
Plot while solving	Off

6.1. Direct (UMFPACK)

Solver type: Linear system solver

Parameter	**Value**
Pivot threshold	0.1
Memory allocation factor	0.7

6.2. Time Stepping

Parameter	Value
Times	range(0,0.1,8)
Relative tolerance	0.01
Absolute tolerance	0.0010
Times to store in output	Specified times
Time steps taken by solver	Free
Maximum BDF order	5
Singular mass matrix	Maybe
Consistent initialization of DAE systems	Backward Euler
Error estimation strategy	Include algebraic
Allow complex numbers	Off

6.3. Advanced

Parameter	Value
Constraint handling method	Elimination
Null-space function	Automatic
Automatic assembly block size	On
Assembly block size	1000
Use Hermitian transpose of constraint matrix and in symmetry detection	Off
Use complex functions with real input	Off
Stop if error due to undefined operation	On
Store solution on file	Off
Type of scaling	Automatic
Manual scaling	
Row equilibration	On
Manual control of reassembly	Off
Load constant	On
Constraint constant	On
Mass constant	On
Damping (mass) constant	On
Jacobian constant	On
Constraint Jacobian constant	On

7. Postprocessing

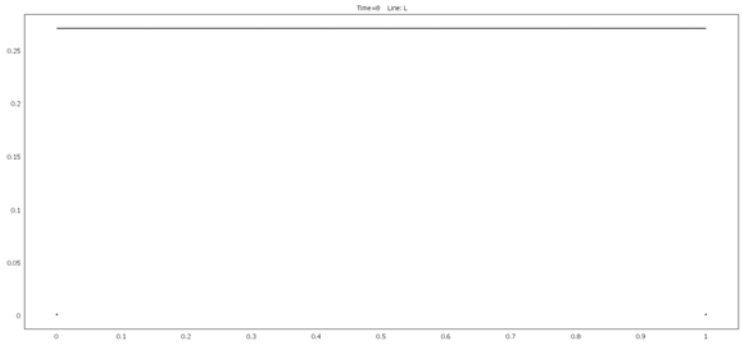

8